Transcriptome-wide functional analysis of post-transcriptional regulatory interactions of the RNA-binding protein HuR/ELAVL1.

Inaugural-Dissertation

to obtain the academic degree

Doctor rerum naturalium (Dr. rer. nat.)

submitted to the Department of Biology, Chemistry and Pharmacy

of Freie Universität Berlin

by

Svetlana Lebedeva

from Moscow

2011

1st Reviewer: Prof. Dr. **Markus Wahl**

Institut für Chemie und Biochemie

Freie Universität Berlin

Takustr. 6

14195 Berlin

Tel.: +49 30 838 53456

E-Mail: mwahl@chemie.fu-berlin.de

2nd Reviewer: Prof. Dr. **Nikolaus Rajewsky**

Department of Systems Biology
Max Delbrück Center for Molecular Medicine
13125 Berlin

Tel.: +49 30 9406 2999

Email: rajewsky@mdc-berlin.de

date of defence: 16.07.2012

Biology

В. Набоков

Муза меня не винит: в науке о трепетах жизни
все - красота. Искромсав осторожно липовый листик,
винт золотой верчу, пока не наметятся ясно
в круглом белом просвете святые зеленые соты;
или же сердцем живым распятой лягушки любуюсь:
сладостно рдеет оно, будто спелая, липкая вишня.
Режу, дроблю, вникаю, вижу сокрытые мышцы,
ветви несметных жил, и, что вижу, мелками цветными
четко черчу на доске.
Сверкают стекла, невнятно
пахнет эфиром и прелью в комнате длинной и светлой.
Радостен тонкий труд, и радостно думать, что дома
ждет меня томик стихов и музой набитая трубка.

Cambridge

My Muse blames me not: in the science of life's flickering movements
Everything is pure beauty. Having carefully dissected a linden leaf,
I turn the golden screw until I see the clear outline
of the sacred green cells in the white circle of light.
Or I admire a living heart of a crucified frog:
it glows red like a ripe cherry sticky with sweet juice.
I cut, mash, inquire and see hidden muscles,
countless branching fibers, and all that I see, I with colored chalks
precisely sketch on a blackboard.
Glitter of glasses, indistinct
smells of ether and mold in the long and bright room.
This fine work is joyful, and as joyful is the thought that at home
my small book of poems and my pipe stuffed by Muse await me.

V. Nabokov

Statement of contributions

This work is the result of a collaborative project. The project was designed and supervised by Nikolaus Rajewsky. Experiments were designed and performed by myself with help of Kathrin Theil. Marvin Jens performed all the bioinformatic analysis presented here, and the corresponding figure panels were made by myself based on raw data plots. Experiments for SILAC and pSILAC proteomics were performed by myself with help of Kathrin Theil, and the mass-spectrometry measurements were performed by Björn Schwanhäusser within the collaboration with the lab of Matthias Selbach. Deep sequencing for the HuR paper was performed in the BIMSB sequencing facility, laboratory of Wei Chen. The HuR paper was written by myself, Marvin Jens, and Nikolaus Rajewsky.

Acknowledgement

My first and great thanks go to my computational *co*-author Marvin Jens, without whom it would have been impossible to handle huge amounts of high-throughput data and whose clear mind was indispensable for distilling grains of sense out of an enormous amount of data.

Nikolaus Rajewsky is absolutely supportive and inspiring supervisor. He taught me several very important things for my career: not only using leading-edge laboratory techniques, but working on interdisciplinary collaborative projects, which was an indispensable experience for my future scientific career.

I thank all other Rajewsky lab members for their valuable input, especially Kathrin Theil, who helped me a lot on the last stage of my project.

We thank Markus Landthaler for a lot of help and valuable ideas. Great thanks go to Björn Schwanhäusser and Matthias Selbach not only for performing the proteomics analyses, but also for useful discussions. We thank the Wei Chen lab, Na Li, Claudia Langnick and Mirjam Feldkamp for help with the sequencing. I thanks Markus Hafner from the Tom Tuschl lab for help with PAR-CLIP.

Many thanks to Ferdinand le Noble and his students Qiu Jiang and Dong Liu for introducing me to the zebrafish model and help with all the fish experiments and discussions.

I thank the Helmholtz association for funding.

Thanks to my mom and all my family and friends for countenance.

Summary

Post-transcriptional regulation is performed by small RNAs and RNA-binding proteins (RBPs) which control mRNA splicing, export, degradation and translation efficiency. Each small RNA and RBP interacts with up to thousands of target transcripts, but only for a few RBPs their targets have been comprehensively identified.

HuR/ELAVL1 is a conserved RBP which regulates mRNA stability and translation. The aim of the present collaborative work was to characterize functional targets of HuR. To obtain precise transcriptome-wide binding sites of HuR in human cells, we used crosslinking and immunoprecipitation (IP) coupled with deep sequencing of bound RNA. The functionality of these sites was validated by measuring the transcriptome-wide impact of HuR knock down on mRNA levels. We also measured changes in protein synthesis of thousands of proteins which reflected the role of HuR in protein synthesis. We found multiple binding sites of HuR in introns and shown a role of HuR in mRNA processing. We also discovered the unexpected regulation of the microRNA miR-7 by HuR.

In summary, we identified thousands of direct and functional HuR targets, found a human miRNA controlled by HuR, and propose a role for HuR in splicing.

Zusammenfassung

Posttranskriptionelle Regulation erfolgt durch RNA-bindende Proteine (RBPs) und kleine RNAs, welche Prozessierung (Splicing), Export, Degradation und Effizienz der Translation der mRNA ausführen. Die neuen Hochdurchsatz-Technologien und bioinformatische Analyse/Vorhersagen zeigen, dass jede kleine RNA oder RBP tausende von mRNAs kontrollieren kann. Dennoch wurden bisher nur für wenige RBPs die Ziel-mRNAs vollständig identifiziert.

Das RBP HuR/ELAVL1 ist evolutionär konserviert und kontrolliert die Stabilität und Translationseffizienz von mRNAs. Das Ziel dieser Arbeit ist die Identifizierung und Charakterisierung von funktionellen Ziel-mRNAs von HuR (auf Transkriptoms-Ebene). Um transkriptomweit die präzisen Bindestellen von HuR in humanen Zellen zu identifizieren, haben wir UV-licht induzierte Querverbindung und Immunoprezipitation von HuR, gefolgt von Sequenzierung, angewendet. Die Auswirkung von HuR-*knock down* auf die mRNA-Pegel validierte die Funktionalität der identifizierten Bindungsstellen. Wir haben die Wirkung von HuR auf die Änderung der Proteinsynthese von tausenden von Proteinen gemessen, was die Rolle von HuR in der Synthese der Proteinen reflektiert. Wir haben mehrere Bindestellen von HuR in Introns identifiziert und eine Rolle von HuR in mRNA-Prozessierung gezeigt. Zusätzlich haben wir eine

unerwartete Rolle für HuR in der Prozessierung von miR-7 aufgedeckt.

Zusammenfassend, wir haben tausende von direkten und funktionellen HuR Ziel-mRNAs identifiziert und eine Rolle von HuR im alternativen Splicing undin Prozessierung von miR-7 aufgedeckt.

Table of contents

1. Introduction

1.1. Post-transcriptional regulation.

In prokaryotes which lack a nuclear envelope, transcription is directly coupled to translation. Translated RNA cannot be degraded, because translation starts on nascent mRNA before the transcription is complete. In contrast, eukaryotic mRNA goes through a number of post-transcriptional processing steps before entering active translation. Eukaryotic mRNA is capped, polyadenylated and spliced, it can be edited, and it has to be exported from the nucleus. In the cytoplasm, it can immediately enter translation or be stored in a translationally inactive form, transported to another cytoplasmic compartment or degraded by dedicated proteins. All of these processes contribute to the amount of protein finally produced from the mRNA and result in a discrepancy between mRNA and protein levels in eukaryotes. The correlation between protein and mRNA levels has been measured several times in eukaryotes and it is decreasing with the increase in organism complexity (R^2~0.8 in *E.coli [1]*, 0.6 in yeast [2] and R^2~0.4 in human [3]).

It may seem that this amount of post-transcriptional processing *per se* should prolong the time between transcriptional activation and start of protein production. Counterintuitively, however, many post-transcriptional processes speed up gene expression. Capping and polyadenylation are necessary for translation, non-capped transcripts and transcripts with short poly(A) tail are inefficiently translated and rapidly degraded. Spliced genes are expressed more effectively than intronless genes; splicing facilitates mRNA export and increases quality control via nonsense-mediated decay (NMD) [4]. Splicing also enhances translation [5]. Storing mRNA after transcription allows to bypass the transcriptional activation step when a fast response is needed. On the other hand, alternative splicing (AS) creates isoform diversity by changing coding sequence (and thus the encoded protein) or the regulatory regions (5' and 3' untranslated regions, UTRs, which contain most regulatory sequences of mRNAs). Post-transcriptional regulation (PTR) accounts for protein production when transcription is not functional or not possible. For example, early embryonic development of most animals completely relies on post-transcriptional regulation, because embryos are transcriptionally silent during the first few cell divisions. Transport of mRNA and localized translation accounts for protein production on a long distance from the nucleus in dendrites and axons of neurons [6]. Additionally, RNA editing can change the splicing pattern, localization and stability of mRNAs [7]. Thus, all of these processes of post-transcriptional regultaion increase the dynamic range and flexibility of gene expression.

The known trans-acting factors of PTR are RNA-binding proteins (RBPs) and small non-coding

RNAs which bind cis-regulatory sequence elements of mRNAs. Most of the known regulatory sequences are located in 3'-untranslated regions (3'UTRs), which are comparable in length to coding regions and often bear regulatory elements for many RBPs and miRNAs simultaneously. On the other hand, there are over 600 [8] miRNAs (the main class of small RNA regulators) and around 700 RBPs in the human genome, many of which target hundreds of transcripts ([9] [10] [11] [12-14]). Thus, although most miRNAs and RBPs as well as their targets are restricted to certain cell types, there is still a large amount of combinatorial action between post-transcriptional regulators. Changing the 3'UTR by alternative splicing or alternative polyadenylation will change the mRNA fate by defining which of the regulatory elements will be present in the transcript [15]. The combination of RBPs and miRNPs on the 3'UTR which defines the post-transcriptional output of the gene is often referred to as the "post-transcriptional regulatory code". Jack Keene put out a hypothesis of "RNA regulons" posing that mRNAs coding for proteins which belong to one complex or pathway should bear similar combinations of regulatory elements. They will be processed and translated together, and the newly synthesized proteins will immediately form the functional complex [16].

The contribution of PTR to net expression of a gene is variable. Many of the PTR effectors seem to only slightly modulate gene expression, playing rather a buffering role and safeguarding against leaky transcription [17] . However, miRNAs or RBPs also can serve as master regulators leading to a dramatic switch of developmental programs. For example, miR-430 eliminates maternal transcripts in the zebrafish embryo during maternal-to-zygotic transition [18]. The first miRNAs discovered in *C. elegans*, lin-4 and let-7, control developmental timing. The RNA-binding protein Sex-lethal (Sxl) controls sex determination in *Drosophila* by alternative splicing of its targets [19].

1.1.1. RNA-binding proteins (RBPs).

There are approximately 700 RBPs annotated in the human genome. Remarkably, most of this diversity is generated by combinations of a relatively small number (~10) of highly conserved RNA-binding domains (RBDs) [20]. Each individual RBD usually binds only a few bases, conferring only modest sequence specificity of binding. Therefore most RBPs comprise more than one RBD (on average four [20]). Combination of multiple RBDs creates a modular structure which: 1) increases affinity of RBPs to their targets 2) at the same time allows easy remodeling of RBP complexes by having several relatively weak interactions instead of a single strong interaction 3) allows one RBP molecule to recognize and bind several RNA molecules. Together with generally low sequence specificity of many RBPs, the modular structure of RBPs ensures the dynamic nature of RNP complexes.

Interestingly, however, the number of known RBPs is likely underestimated, and novel RNA-binding domains are still being discovered. For example, more and more metabolic enzymes like GAPDH [21] are now shown to bind and regulate RNA [22].

1.1.2. Animal microRNAs.

Small RNAs are non-coding RNAs ~20-30 nt long. They were discovered in 1993 [23] and are now described in numbers of hundreds to thousands in animals and plants. Small RNAs can originate by

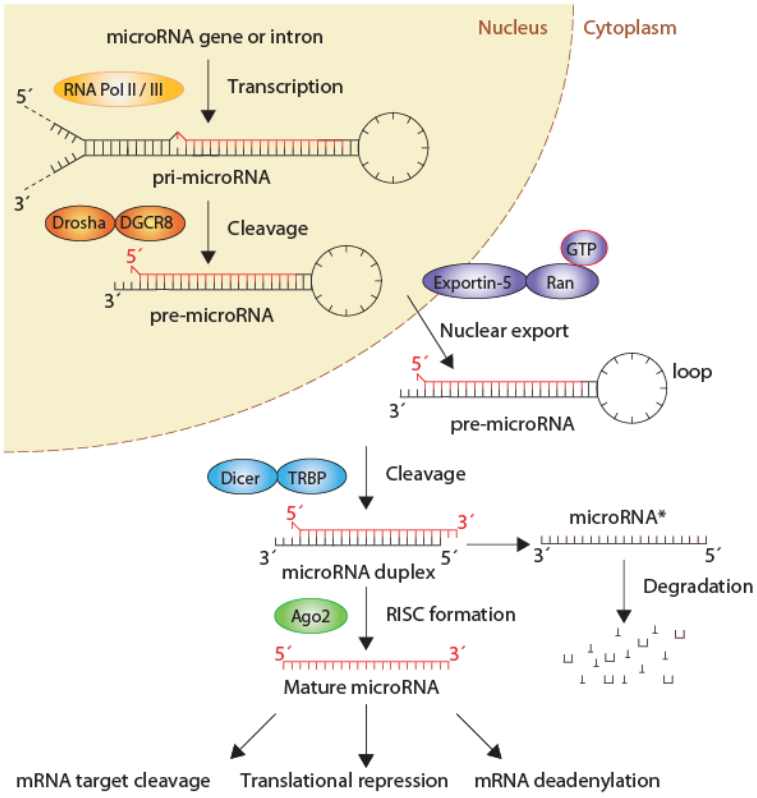

Figure 1. Animal microRNA biogenesis (modified from [20] with permission)

MiRNA primary transcripts (pri-miRNA) are encoded as parts of introns or as independent transcription units and are mostly transcribed by RNA polymerase II. The double-stranded hairpin precursor (pre-miRNA) is cleaved out of the primary transcript by the Microprocessor complex (comprising RNase Drosha and its cofactor DGCR8). Pre-miRNA is transported into the cytoplasm by Exportin-5. A cytoplasmic processing complex containing the RNase Dicer cleaves a double-stranded duplex out of the hairpin. The duplex is then unwound and one of the strands (mature miRNA, or guide strand) is incorporated into the Argonaute protein to form the functional RISC (RNA Induced Silencing Complex). RISC induces silencing of target mRNAs by cleaving the target mRNA or inducing its degradation and/or translational repression. The other strand (star strand) is degraded.

several different pathways, but all of them are bound by proteins of the PIWI/Argonaute (Ago) family, to act together as the small RNA effector complex. Ago proteins are present in archaea and all eukaryotes [24]. The small RNPs are guided by the small RNA to target sites in mRNA with perfect or partial complementarity. Most often small RNA-induced silencing results in target cleavage and degradation, or deadenylation and translational repression [25].

MiRNAs are the best understood class of endogenous small RNAs. MiRNAs are encoded in the genome as part of introns of protein-coding genes or as independent long non-coding transcripts. The generation of miRNAs from these precursor transcripts occurs in two steps (Figure 1) [26]. First, a ~70nt double-stranded pre-miRNA hairpin is cut out of the primary transcript by a complex of the RNase Drosha and its cofactors. This pre-miRNA is exported into the cytoplasm and cut by the RNase Dicer/TRBP into a ~21nt-long duplex with 2nt 3'overhangs and a loop sequence (which is degraded). One strand of the duplex (mature miRNA) is then loaded into one of the four (in human) Argonaute proteins to serve as a guide strand. The other strand which is called star, or passenger strand, is degraded. Loaded Argonaute protein with additional factors forms the functional RISC (RNA Induced Silencing Complex).

The RISC complex is guided by RNA-RNA complementarity of the miRNA to the target mRNA. In animals, most miRNAs form Watson-Crick basepairs with their targets within the first 7-8 nt of the 5' end (this region of the miRNA is called “seed sequence”), supported by a few more base pairs in the 3' end of the miRNA. RISC binding to target mRNAs results in deadenylation of mRNA leading to degradation or translational repression (see below). Perfect complementarity of miRNA and the target leads to target cleavage, however, this mode of action is rare among animal miRNAs.

Computational tools are widely used in miRNA research. For example, Dicer processing pattern is implemented in the miRDeep algorithm for discovery of novel miRNAs from next generation sequencing data [8; 27] . Many important seed-complementary target sites in the 3'UTRs are evolutionary conserved. This property is used to predict miRNA targets by several algorithms, such as PicTar [9; 10] and TargetScan [11] .

1.1.3. Translation and mRNA stability control by RBPs and miRNAs.

Most protein-coding mRNAs posess two main stability and translation determinants: the 5' cap and the poly(A) tail. These structures protect mRNA from nucleolytic degradation from the 5' and 3' ends, respectively. The cap is bound by the cap-binding protein EIF4E and the poly(A) tail by the poly(A)-binding protein (PABP). Moreover, the cap-binding complex and PABP physically interact, closing actively translating mRNA into a loop to stimulate re-initiation of translation [28] .

Deadenylation of mRNA is the first step to trigger mRNA decay. As a consequence of deadenylation, the translation loop is disrupted and the 3' end is made accessible to the exosome (a protein complex containing several proteins with 3'→5' exonucleolytic activity). Deadenylation is also necessary for decapping, which leads to degradation in the 5'→3' direction, by the exonuclease XRN. Endonuceolytic cleavage in the body of mRNA can trigger degradation by exonucleases in both directions (see also a recent review [4]).

The general mechanism of silencing by animal miRNAs relies on translational repression and mRNA degradation via deadenylation and decapping. The relative contribution of these two processes in miRNA-mediated decay varies for individual miRNA targets (see [29] [30] for review). It is not clear what determines whether the mRNA would be preferentially translationally silenced or degraded, and it is further complicated by the interconnection between these two processes. Deadenylation *per se* can lead to translational silencing and not necessarily to degradation: storage of deadenylated translationally silenced mRNAs is a common mechanism, for example, during oogenesis [6]. On the other hand, translational disruption of an mRNA can trigger degradation of this mRNA independently of miRNA action.

Several groups including our own have attempted to assess the relative contribution of mRNA degradation and translational repression in miRNA-induced silencing on a genome wide scale. These studies used quantitative proteomics [31] and ribosome profiling [32] to quantify changes in protein synthesis for thousands of proteins upon knockdown or overexpression of a miRNA. These studies concluded that for most miRNA targets, miRNAs induce both mRNA degradation and repression of translation, although to a relatively mild degree. Interestingly, a recent study on a single cell level [33] showed that individual targets can be very strongly translationally repressed, depending on the level of the miRNAand the target mRNA.

MiRNA-mediated repression requires proteins of the TNRC6/GW182 family [34]. These proteins directly interact with Argonautes and recruit deadenylases to the miRNA target mRNAs [35] . The GW182 proteins form P-bodies, cytoplasmic aggregates of mRNA degradation factors (CCR4/NOT deadenylase, decapping enzymes and XRN exonuclease) which also contain miRNA-target complexes. Interestingly, miRNA-dependent mRNA degradation is not restricted to P-bodies, and can also take place in the cytoplasm. On the other hand, some miRNA targets can apparently be stored in P-bodies in a translationally silent state without being degraded, to be later readenylated and reactivated [36].

RBPs can affect both mRNA stability and translation through a variety of regulatory sequences situated mostly in the 3'UTR but also in the 5'UTR. One of the best understood examples of such

elements are the socalled AU-rich elements (AREs), sequences in 3'UTRs composed of stretches of U-rich sequences which often contain (AUUUA) repeats [37]. AREs contribute to mRNA instability via the action of multiple destabilizing ARE-binding proteins (AUBPs), for example AUF1, KSRP, BRF, TTP, RHAU, TIA-1, TIAR [4]. AUBPs utilize different mechanisms to regulate ARE-containing RNAs. For example, KSRP and TTP seem to directly recruit the exosome to ARE-containing mRNAs by protein-protein interactions [38], while other AUBPs recruit deadenylase (PARN) [4]. PUM protein bnding induces a structure switch in its target p27 3'UTR, opening up the binding sites for miR-221/222, which leads to silencing of p27 expression [39]. TTP and BRF probably shuttle their targets to P bodies for degradation [40]. On the other hand, HuR and other Hu/ELAV family proteins are the only AUBPs known to stabilize ARE-containing mRNAs. They probably do so by competing away destabilizing proteins [41] and/or changing localization of transcript from P bodies to polysomes [36].

RBPs are also crucial for translational regulation. It is long known that 3'UTR-binding proteins Bruno, Pumilio, Smaug and Bicoid repress translation of their target mRNAs *oskar, nanos, hunchback* and *caudal* in the *Drosophila* embryo. These proteins act by forming an inhibitory loop, sequestering the cap within an inhibitory protein complex and preventing translation initiation [42]. In developing oocytes of *Xenopus*, CPEB protein binds to the cytoplasmic polyadenylation element (CPE) in the 3'UTR of the *cyclin B1* mRNA [43]. CPEB regulates the translational status of *cyclin B1* via the length of the poly(A) tail by recruiting either a deadenylase or a poly(A) polymerase. Of interest, *Xenopus* Elr proteins, homologs of ELAV, participate in the asymmetrical localization and translational silencing of the vegetal pole mRNAs [44].

Post-translational modifications of RBPs can change their effect on mRNA stability and translation. This mechanism can be used to rapidly adapt to changes in the environment. Phosphorylation of an RBP can change its affinity to different target RNAs, affect its cellular localization or change its protein-protein interaction partners. For example, phosphorylation-dependent association of 14-3-3 proteins with HuR [45] and TTP [46] changes their effect on mRNA stability. Conformational changes upon phosphorylation of AUF1 cause its dissociation from the target *GM-CSF* mRNA [47]. Another example of RBP remodeling is the regulation of *p21* and *myogenin* mRNAs by KSRP. In the course of muscle differentiation KSRP is phosphorylated by p38 MAPK and dissociates from these mRNAs [48] which can now be stabilized by HuR [49]. Remodeling of RNP complexes containing HuR protein can occur as a result of post-translational modifications induced by stress. For example, upon UV irradiation HuR binding to *CCND1* mRNA decreases and allows this mRNA to associate with AUF1 [50]. Binding of HuR to *CytC* mRNA decreases upon ER stress, in turn

allowing TIA-1 protein to bind to this transcript [51]. Thus, stabilizing AUBPs compete with destabilizing AUBPs and miRNAs for the target mRNAs, and the sum of the effects will determine the net protein output from the mRNP. Depending on the concentrations of RBPs, miRNAs and their targets in the cell, and on the affinity of the effectors to each target, mRNAs competing for protein factors and miRNAs also potentially affect the degree of post-transcriptional regulation of each other [52].

1.1.4. Interaction of RBPs and miRNAs.

MiRNAs and RBPs mutually regulate each other, adding another feedback layer to the post-transcriptional regulatory network. Most RBPs are regulated by miRNAs and RBPs on the level of their mRNAs, and many RBPs autoregulate their own messages. RBP transcripts tend to have short half-lives which generally correspond to longer 3'UTRs [3], which are more likely to bear miRNA seeds and RBP binding sites.

Often a miRNA is co-expressed in the same tissue with its targets, but the targets are not repressed. This can be due to the presence of RBPs that counteract, directly or indirectly, miRNA-mediated silencing. This type of modulation of miRNA action by RBPs is target-specific. Several RBPs are known to interfere with miRNA action by binding to the same 3'UTR. The DND1 protein binds U-rich sequences in the 3'UTR of *p27* mRNA to prevent binding of miR-221 [53]. In zebrafish embryos, miR-430 is involved in the elimination of maternal mRNAs [18]. However, in primordial germ cells, DND1 protects *nanos1* and *TDRD7* from degradation by miR-430 [53]. APOBEC3G is shown to translationally derepress targets of multiple miRNAs driving them out of P-bodies and into polysomes [54]. HuR protein has been known to counteract miRNA-mediated repression of *CAT-1* mRNA [36]. *CAT-1* mRNA is translationally silenced by miR-122 in hepatocytes. Following amino acid starvation stress it is relocalized from P-bodies to polysomes in an HuR-dependent way. [36]. HuR over expression in cancer cells counteracts miR-548-dependent translation repression of *TOP2A* mRNA, which also involves the relocalization of the mRNA out of P bodies [55].

For some miRNA targets, on the opposite, binding of miRISC is dependent on an auxiliary RBP. Binding of an RBP can change the local secondary structure such as to make the miRNA target site accessible to RISC binding. For example, PUM protein binding opens miR-221/222 binding sites on the *p27* 3'UTR [39]. A similar mechanism may be involved in HuR-dependent repression of *MYC* by let-7 [56] and of *RhoB* by miR-19 [57].

On the other hand, if a RBP affects miRNA processing, this will impact all targets of this miRNA in the tissue where the RBP is expressed. For example, LIN28 binds to the loop of let-7 to block its

processing [58] [59]. HNRNPA1 is required for processing of miR-18a [60]. The splicing factor SF2/ASF regulates Drosha cleavage of miR-7 independently of its function in splicing [61].

Another interesting case of regulation of RBP by miRNA interaction is miR-328/hnRNPE2. The miR-328 sequence mimics a binding site of hnRNPE2.Where miR-328 is expressed, it sequesters hnRNPE2 and relieves translational repression of hnRNPE2 targets [62].

1.1.5. Regulation of alternative splicing by RBPs and miRNAs.

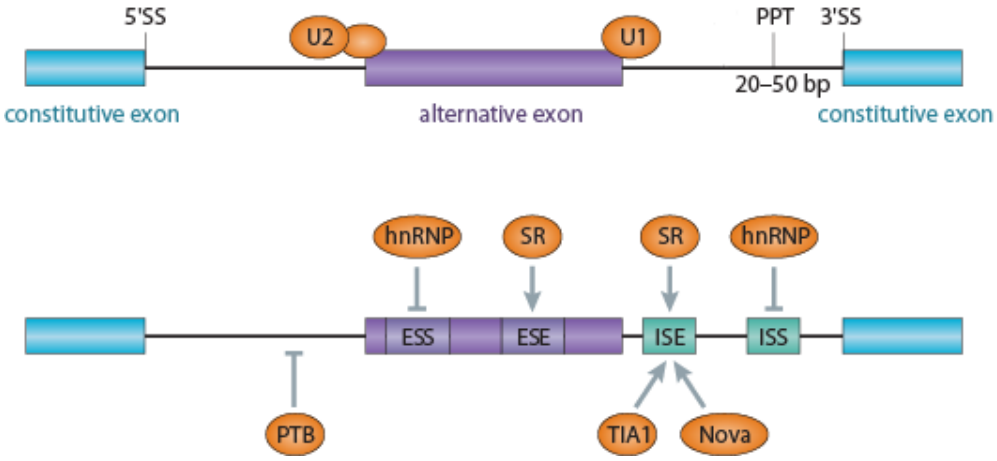

Figure 2, modified from [81], with permission. Determinants of constitutive and alternative splicing. Two constitutive exons (turquoise boxes) flank an alternative exon (purple box). Shown are the U2 snRNP complex binding to the 3' splice site (3'SS) and U1 snRNP bound to the 5'SS. The polypyrimidine tract (PPT) is situated upstream of the 3'SS and is a stretch of U and C nucleotides ~20-50 nt long bound by U2 auxiliary factors. *(above)* Exonic splicing silencers (ESS) and intronic splicing silencers (ISS) are bound by hnRNP family proteins which inhibit splicing. Exonic and intronic splicing enhancers (ESE, ISE) are bound by SR family proteins which promote splicing. A few examples of additional AS regulators are shown: polypyrimidine tract binding protein (PTB), TIA-1 protein, which is also involved in stress granule formation, and Nova protein, which regulates brain-specific patterns of AS. *(below)*

Alternative splicing (AS) is one of the major sources of transcriptome and proteome diversity. AS is an important target for post-transcriptional regulation by multiple RBPs. A decision of whether an exon will be spliced in or skipped is made at the first step of the spliceosome formation. In mammals, due to substantial intron lengths, splicing acts through exon definition (exons are recognized by the splicing machinery first). Exon recognition is performed by U1 snRNP which

binds to the 5' splice site (5'SS) and U2 snRNP which binds with help of U2 auxiliary factor (U2AF) upstream of the exon close to the 3' splice site (3'SS) (Figure 2, above). Interfering with either of these recognition steps would cause skipping of the alternative exon. On the other hand, RBP-assisted recruitment of the splicing machinery to weakly defined splice sites would promote exon inclusion. These two events are the most common cases of alternative splicing in mammals [63]. Regulatory sequences in an alternative exon and the surrounding introns which are recognized by RBPs are called splicing enhancers or silencers. The two most common splicing RBP families are serine-arginine rich (SR) proteins, which promote splicing of alternative exons, and hnRNP proteins that mainly inhibit it. They bind intronic and exonic splicing enhancers or silencers, respectively (Figure 2, below). Interestingly, many RBPs that localize both to the nucleus and cytoplasm have double functions: in the nucleus they regulate AS and in the cytoplasm mRNA stability. Good examples are AUBPs like TIA-1, TTP and neuronal ELAV proteins. Specifically, binding of TIA-1 to U-rich sequences close to the 5'SS promotes AS [64]. Neuronal ELAV proteins bind to the U-rich sequences in introns, blocking recruitment of the U1 RNA [65].

MiRNAs can regulate splicing ndirectly by targeting the mRNAs of many splicing proteins, but no direct binding of RISC complexes to splice sites has been shown so far. However, Argonaute proteins are known to be imported into the nucleus, and nuclear Agos are loaded with miRNAs [66]. A number of miRNAs are specifically enriched in the nucleus compared to the cytoplasm [67]. In addition, siRNAs targeting exon-intron junctions in pre-mRNAs can modulate splicing [68]. Taken together, this allows for an intriguing possibility of direct regulation of AS by miRNAs.

1.1.6. The RNA-binding protein HuR.

The human RNA-binding protein HuR (ELAVL1) is one of the mammalian homologs of the *Drosophila* protein ELAV (Embryonic Lethal, Abnormal Vision). ELAV proteins are highly conserved: they seem to be present in all main phylogenetic groups of metazoans [69]. ELAV proteins consist of three consecutive RRM-type RNA-binding domains (Figure 3A). The first two

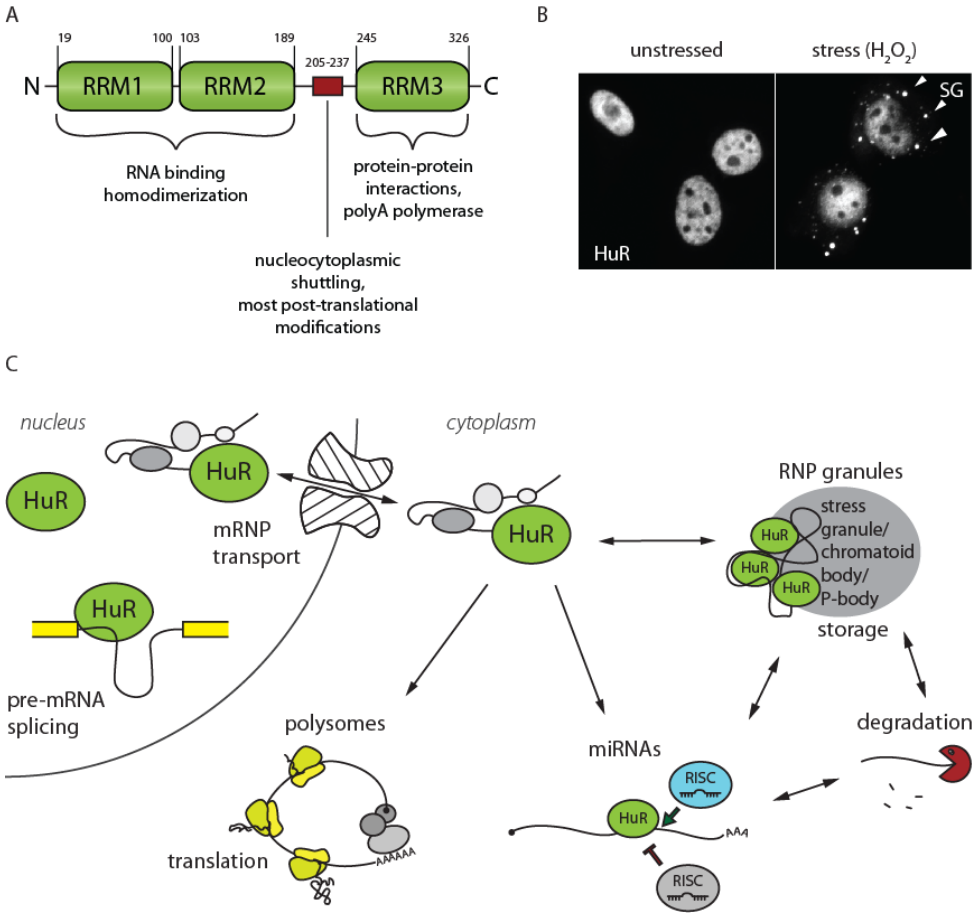

Figure 3. Composition and functions of the HuR protein.

(A) HuR protein structure. HuR comprises three RNA recognition motifs (RRMs). RRM1 and RRM2 are binding target RNA. RRM3 is probably binding and elongating poly(A) tails and participates in protein-protein interactions. The linker between RRM2 and RRM3 contains a nucleocytoplasmic shuttling domain and the sites of most post-translational modifications. (B) HuR localization. Immunostaining of HuR in unstressed HeLa cells (left) shows predominantly nuclear localization. Upon oxidative stress (right), HuR is partially relocalized to the cytoplasm and stress granules (SG, arrowheads). (C) HuR protein shuttles between the nucleus and the cytoplasm. In the nucleus HuR participates in pre-mRNA processing and export of the pre-mRNPs. In the cytoplasm, HuR mainly protects mRNAs from degradation, enhances translation of mRNAs, modulates effects of miRNAs and shuttles mRNPs in and out of cytoplasmic granules.

domains, RRM1 and RRM2, act in tandem to bind uridine-rich sequences in the target RNA. The 63 amino acid long linker separates RRM1-RRM2 tandem from RRM3. The linker includes the sites of most post-translational modifications and contains a non-canonical nucleocytoplasmic shuttling signal [70; 71]. RRM3 seems to be dispensable for RNA binding [72]; it might participate in protein-protein interactions [73] and has a reported poly(A) polymerase activity [74]. HuR is ubiquitously expressed [75] and its knockout is embryonic lethal both in *Drosophila* [76] and in mouse [77]. HuR has been implicated in multiple and diverse processes such as embryonic development [77], differentiation [78] [79] [80], cell proliferation [81-83], inflammation [84] and stress response [85-87]. In unperturbed cells HuR is predominantly localized in the nucleus (Figure 3B), but in contrast to neuronal ELAVs, which regulate alternative splicing of their targets, HuR has only been shown to bind to a single exon (exon 6 of the apoptosis receptor FAS), coregulating its splicing together with TIA proteins [88]. Various stimuli like stress or developmental signals change the nuclear/cytoplasmic ratio of HuR (Figure 3C). HuR translocation to the cytoplasm is governed by post-translational modifications, mainly phosphorylation by PKC [89] , MAPK [90] and Chk2 [91]. In the cytoplasm HuR binds to 3'UTRs of its target mRNAs to stabilize them and activate their translation (Figure 3C) (reviewed in [92]). Interestingly, HuR has been described to also bind 5'UTRs to regulate translation of *IGFIR* [93] and *HIF1A* mRNA [94].

HuR targets are often (but not exclusively) the so-called “immediate response genes”. These genes are rapidly activated in response to stress (for example, heat shock proteins) or inflammatory stimulus (interleukins). HuR also regulates cell cycle genes (cyclins and CDK inhibitors [81] [86] [95]) and is associated with increased cell proliferation [96]. Many cancers exhibit elevated HuR expression [97], and inhibition of HuR function slows down cancer cell proliferation [82].

HuR is associated with cytoplasmic RNP granules. Stress granules (SG) [98] (Figure 3B) are aggregations of stalled translation initiation complexes which appear when translation is arrested upon cellular stress (heat shock, oxidative stress and others). The bulk of cellular mRNA is sequestered from translation in SG, and only specific mRNAs needed for stress response are being translated. HuR is localized to stress granules (Figure 3C, [85]) but is also known to stabilize many transcripts of stress response genes in the cytoplasm. Another type of RNP granule, the chromatoid body in developing spermatids, also accumulates HuR. At later stages of spermatocyte development, HuR translocates to polysomes together with its target mRNAs to promote their translation [99]. HuR/ELAV is essential for spermatid differentiation in mammals [78], and this function is conserved in flatworms [69].

1.2. Immunoprecipitation-based methods to study RNA-binding proteins.

To define unknown RNA targets of an RBP, methods have been developed which are based on immunoprecipitation (IP) of RBP-RNA complexes (RIP). RNA is isolated from the IPand then analyzed, traditionally with microarrays (RIP-Chip), or, more recently, with high-throughput sequencing (RIP-Seq). However, the necessity to preserve RNA-protein interactions demands mild washing conditions during IP. This may lead to co-precipitation of interacting proteins and associated RNAs, thus detecting indirect interactions. Dependent on the conditions, even reassociation of RNA-protein complexes after lysis is possible [100]. Nevertheless, if performed carefully, the RIP method has been a useful tool for defining confident targets of RBPs [101]. However, another important technical limitation of RIP-based methods is the inability to precisely identify binding sites of the RBP on the mRNA.

Together with IP, crosslinking of nucleic acids to proteins can be used. It has two main advantages: 1) it allows more stringent washing to reduce background and remove non-specific interactions and 2) the crosslinked nucleotides mark the sequence which directly interacts with the protein. Chemical crosslinking with formaldehyde, which is widely used for DNA-protein crosslinking, is possible for RNA [102], but it results in large complexes of RNA and proteins crosslinked to each other, which reduces specificity. Chemical treatment also damages RNA, which could interfere with sequencing. Therefore UV light is used to crosslink RNA. UV light is readily absorbed by nucleobases and induces RNA-RNA and RNA-protein crosslinks. In the latter case, only bases which are in close contact with the protein will be crosslinked, allowing to precisely identify protein binding site. Traditionally, high energy UV light of 254nm is used. The drawbacks of UV crosslinking, such as low crosslinking efficiency, RNA damage and RNA-RNA crosslinks, reduce the amount of recovered protein-RNA complexes.

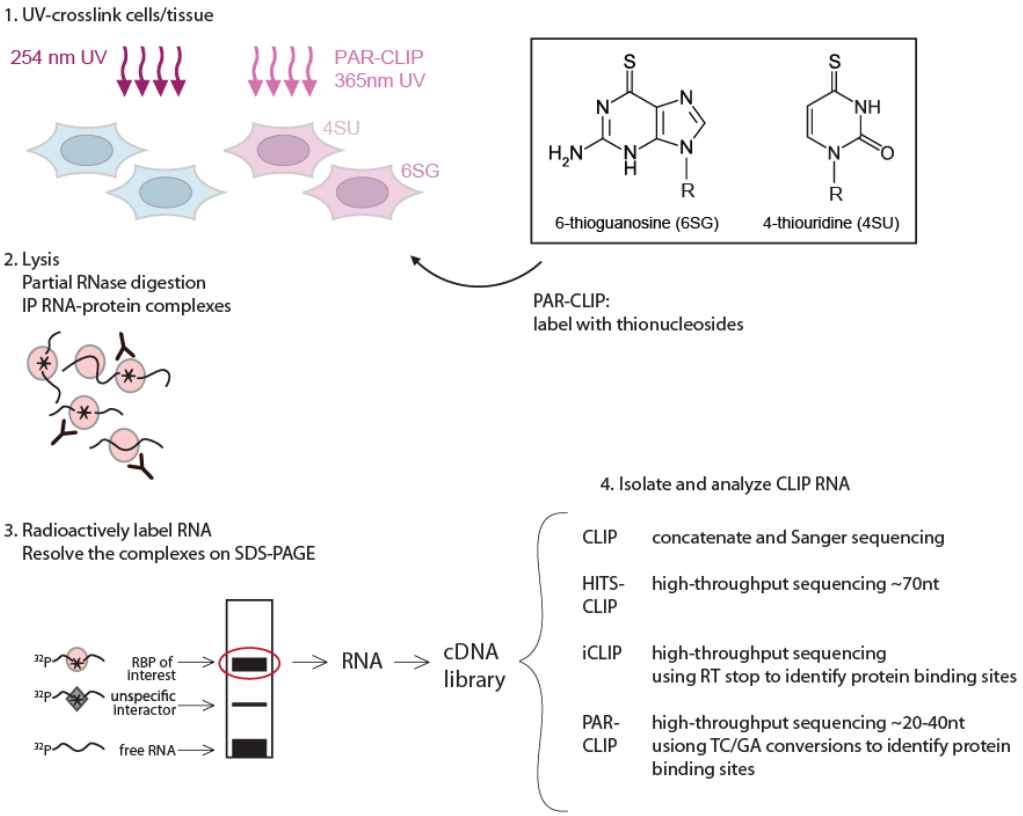

Method	Description	Reference
CLIP	The original method based on UV-crosslinking and immunoprecipitation.	[81]
HITS-CLIP	The first use of high-throughput sequencing together with CLIP.	[82]
iCLIP	Uses the property of the reverse transcriptase to terminate at crosslink sites. Identifies RBP binding sites with nucleotide resolution.	[1]
PAR-CLIP	Uses photoactivatable nucleosides to enhance crosslinking efficiency. Nucleotide conversions allow identification of RBP binding site with nucleotide resolution.	[12]

Figure 4. Summary of the recent crosslinking and immunoprecipitation (CLIP) methods.

(1) Cultured cells or isolated tissues are UV-irradiated to crosslink RNA to proteins. In PAR-CLIP, photoreactive thionucleosides (insert) are incorporated into RNA by metabolic labeling prior to crosslinking. Low energy UV light of 365nm is used in PAR-CLIP so that only thionucleosides and not regular nucleotides are crosslinked. (2) Crosslinked cells are lysed, RNA is partially digested to yield short RNA tags, and the complex of the protein of interest crosslinked to RNA is pulled down. If an antibody against endogenous protein is not available, a tagged version can be expressed and pulled down with an antibody against the tag. (3) After washing, the crosslinked protein-RNA complex is radioactively labeled, boiled in SDS and resolved on a denaturing gel. The band corresponding to the molecular weight of the protein of interested is cut out. This step greatly reduces the background of unbound RNA and unspecific interactors. (4) RNA is isolated from the gel using proteinase K and phenol extraction. Adapters are ligated to the RNA, and after PCR amplification, the cDNA library is analyzed by sequencing.

Several modifications of the CLIP (CrossLinking and ImmunoPrecipitation of RBPs) method have

recently been developed. The first CLIP protocol was developed in the Darnell lab [103] (Figure 4). After UV irradiation, cells or tissues are lysed, and the lysate is mildly treated with RNase, for example, RNase T1. This treatment creates short RNA fragments crosslinked to proteins. RNA-protein complexes are then purified using an antibody against the protein of interest. If the antibody against endogenous protein is not available, tag-assisted purification of expressed protein is an efficient alternative. Immunoprecipitated complexes are then separated from co-purifying contaminants and free RNA on an SDS-PAGE gel. Protein is removed by proteinase K, and the crosslinked RNA fragments are recovered by phenol extraction and precipitation. A common strategy is to ligate adapters to the isolated RNA and PCR amplify the library. In the original CLIP method, the tags were then concatenated and sequenced by conventional sequencing. Later, HITS-CLIP (for High Throughput Sequencing CLIP) was developed, where CLIP RNA is ligated to sequencing adapters and converted into a next generation sequencing library.

The amino acid which was directly crosslinked to RNA cannot be completely removed by proteinase K, and the reverse transcriptase falls off or inserts a non-cognate nucleotide during reverse transcription through this lesion. This property is implemented in newly developed CLIP methods to identify the precise RBP binding site. A recent approach, termed iCLIP (individual nucleotide resolution CLIP), is based on mapping the nucleotide at which the reverse transcriptase (RT) stopped as the site of RBP-RNA interaction [14].

An technique called PAR-CLIP (PhotoActivatable Ribonucleoside enhanced CLIP) was developed in the Tuschl lab [13]. PAR-CLIP makes use of photoreactive thionucleoside analogues, 4-thiouridine (4SU) and 6-thioguanosine (6SG) (Figure 4, insert), which readily incorporate into newly synthesized RNA if added to the cell culture medium. They are excitated by low energy (365nm) UV light, which minimizes damage to the rest of the RNA. At the same time, the efficiency of crosslinking is greatly enhanced. In addition, thionucleotides, when crosslinked, produce characteristic nucleotide conversions which pinpoint the exact place of protein-RNA contact. 4SU base-pairs with guanine better than with adenine because the sulfur at the 4 position is less electrophylic than oxygen [104]. This tendency is increased for the crosslinked 4SU, which leads to T-to-C substitutions during reverse transcription. By analogy, crosslinked 6SG causes G-to-A conversions. After sequencing and mapping, these nucleotide conversions pile up at the RBP binding site. Importantly, T-to-C and G-to-A mutations also provide an internal control of the PAR-CLIP experiments descriminating truely crosslinked RNA from the background RNA. This is an advantage over the conventional 254nm UV CLIP, because the need for sequencing negative control, such as IgG IP, is eliminated.

The necessity to introduce the photoactivatable nucleosides into the living organism limits the applicability of PAR-CLIP to in vivo studies. Apart from cell lines, this is currently successfully done in the nematode *C.elegans* [133] and has a potential to be introduced in a tissue-specific way in more complex animals like *Drosophila* using the so-called 'TU tagging' system [105].

2. Aims of this thesis

In the cell, RNA is always bound by RNA-binding proteins (RBPs) which participate in the regulation of all aspects of mRNA function. However, the transcriptome-wide effect that a particular RBP has on mRNA stability and translation of all of its targets has not been addressed before. We therefore chose one RNA-binding protein, HuR/ELAVL1, as a case study to systematically characterizing its interactions in the cell.

The objective of this work was to characterize the function of the HuR protein on systemic level. More precisely, we aimed to globally assess the role of HuR on stability and translation of its target mRNAs. For this, we experimentally addressed the following questions:

- To define transcriptome wide binding sites (and target transcripts) of the RNA-binding protein HuR in human cells (using PAR-CLIP)
- To check the functionality of the defined HuR-target interactions by quantifying the effect of HuR knock down:
    - on total mRNA levels (using RNA-Seq)
    - on mRNA alternative splicing changes (using mRNA-Seq)
    - on protein synthesis levels (using SILAC proteomics)
    - on miRNA levels (using small RNA-Seq)

3. Results

3.1. Identification of thousands of endogenous HuR binding sites by PAR-CLIP.

To identify HuR binding sites, we performed PAR-CLIP in HeLa cells using an antibody against endogenous HuR protein (Figure 5A, left panel). Conventionally, PAR-CLIP is performed with 4-thiouridine (4SU) labeling. Although 4SU labeling does not introduce a sequence bias in PAR-CLIP [13], we used alongside with 4SU another nucleoside label, 6-thioguanosine (6SG), in a separate PAR-CLIP experiment. In addition, our proteomics measurements required maintaining cells in special (SILAC) medium. To account for possible gene expression difference between the two media, we used SILAC medium to perform PAR-CLIP with both 4SU and 6SG. For comparison, we also performed a standard PAR-CLIP experiment with 4SU in DMEM. (See Table 1 for the summary of the experiments).

Table 1. Overview of the samples and experiments.

PAR-CLIP of endogenous HuR			
thionucleoside label	normal medium (DMEM)	SILAC medium	
4SU	X	X	
6SG		X	
Gene expression changes after HuR knock down			
	siRNA1	siRNA1	siRNA2
mRNA sequencing	X	X	X
pSILAC (3d)		X	
SILAC (5d)		X	X

Since HuR localization is sensitive to multiple kinds of cellular stresses [106], we confirmed that neither thionucleoside treatment nor growing in SILAC medium caused relocalization of HuR into the stress granules [107].

Details of the PAR-CLIP computational analysis pipeline can be found in [107]. Briefly, RNA isolated from HuR IP was sequenced on Illumina Genome Analyzer (see methods) using the small RNA sequencing protocol (36 bp reads). After adapter removal, sequencing reads were aligned to a set of human pre-mRNA sequences (based on RefSeq annotation). T-to-C and G-to-A conversions were prevalent in the sequencing reads from 4SU and 6SG experiments, respectively, confirming the efficiency of the labeling and crosslinking (Figure 5C,D).

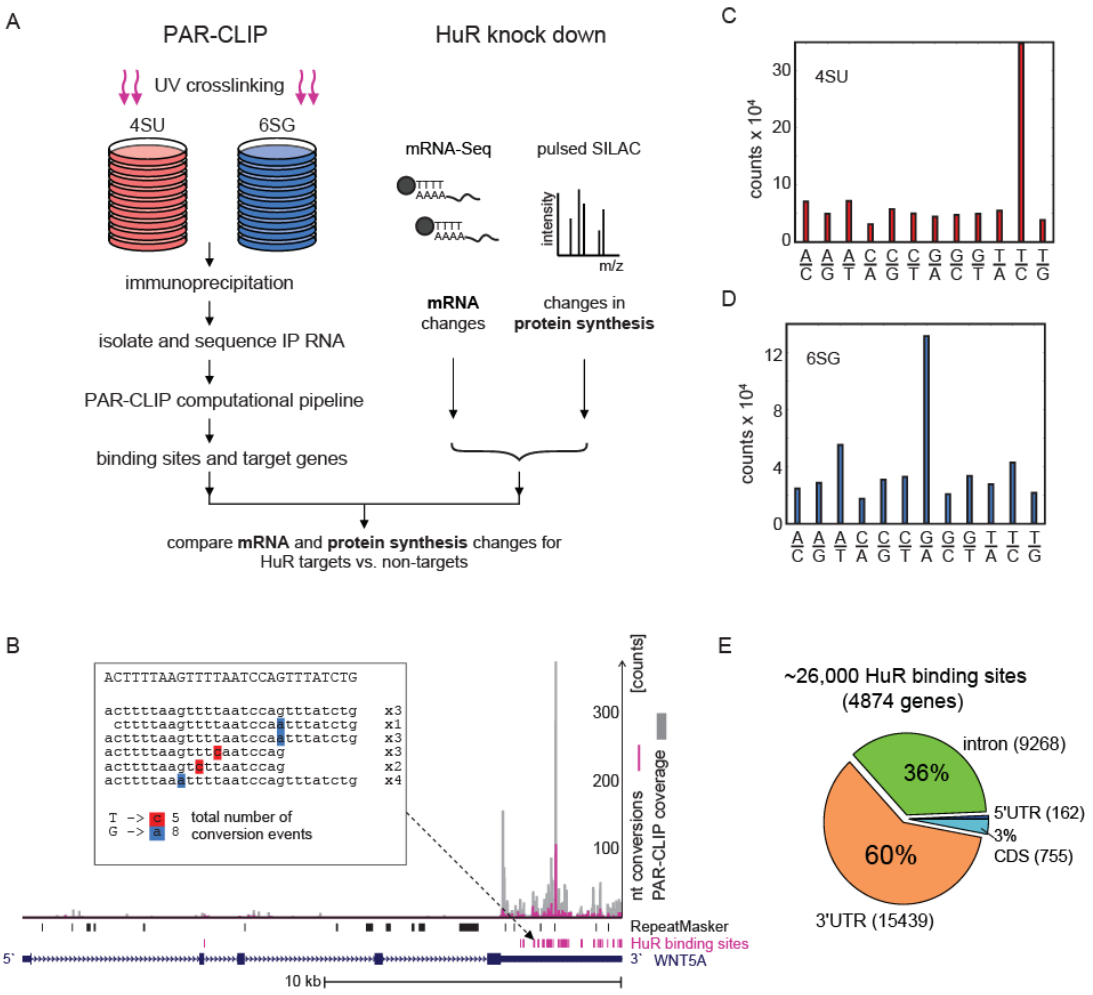

Figure 5. Experimental design and PAR-CLIP of HuR.

(A) Outline of experiments. Transcriptome-wide HuR binding sites are derived from PAR-CLIP of endogenous HuR in HeLa cells labeled with 4-thiouridine (4SU) or 6-thioguanosine (6SG). The effect of HuR knock down on transcript levels was measured by mRNA sequencing (“RNA-seq”) and on protein synthesis by pulsed SILAC shotgun proteomics (“pSILAC”). (B) Representative example of PAR-CLIP data. The coverage by aligned reads (gray) and nucleotide conversions (purple) are shown along the WNT5A gene. HuR binding sites are indicated as purple boxes. Insert: Example of a PAR-CLIP consensus cluster. The WNT5A mRNA sequence is shown in uppercase letters at the top. Aligned PAR-CLIP reads are shown in lowercase with mismatches highlighted (T to C in red for 4SU, G to A in blue for 6SG). xN denotes N counts for a read. (C,D) Elevated numbers of T-to-C conversions in 4SU and G-to-A in 6SG experiments confirm efficient crosslinking. (E) Distribution of HuR binding sites across transcript categories.

RBP binding sites are defined in PAR-CLIP as clusters of overlapping or directly adjacent sequencing reads which contain characteristic nucleotide conversions. We grouped uniquely aligning reads into read clusters (a cluster included adjacent reads and overlapping reads). Each

cluster was given a score based on the number of reads and the number of characteristic nucleotide conversions. Clusters mapping antisense to known transcripts and to the Y chromosome (which is absent in HeLa cells) were used to estimate false discovery rate (see [109] for details). Clusters overlapping repetitive elements were discarded. The average cluster size was small (27-39 nt) corroborating the high resolution of PAR-CLIP. An example of a cluster in a known target gene, WNT5A, is shown in Figure 5B.

We defined our final set of HuR binding sites (which we dubbed "consensus set") by taking clusters that contained reads from at least two out of the three libraries and at least one characteristic conversion. At the cutoff of 5 % FDR, there are ~26000 endogenous HuR binding sites in HeLa cells which belong to ~4800 transcripts (Figure 5E). Additionally, we defined a "conservative set" of target genes, which contained read clusters and conversions from all of the three PAR-CLIP libraries. This set comprised ~1200 high confidence HuR targets.

As expected from the previous knowledge, HuR predominantly bound 3'UTRs (~15000 sites). Surprisingly, one third of the binding sites (~9000) is located in introns, and ~800 genes had HuR binding exclusively in introns. This encouraged us to further investigate possible functions of HuR in pre-mRNA processing (see below).

3.2. Reproducibility and validation of PAR-CLIP.

Since the PAR-CLIP experiments were performed with different nucleoside labels and in different culturing medium, we sought to assess the reproducibility of PAR-CLIP in these conditions. We reassembled HuR clusters taking separately the reads derived from only 6SG or only 4SU libraries (the two 4SU libraries were pooled together) and compared the results for both nucleoside labels to each other and to the consensus target set. The distribution of binding sites across transcript categories was reproduced in both 4SU and 6SG (Figure 6A). 65-74% of the target genes overlapped between the 4SU and the 6SG sets (Figure 6B, left). 78% of 4SU targets from DMEM overlapped with the 4SU targets from SILAC medium (Figure 6B, right).

We compiled a list of HuR targets known from the literature (Appendix). 68 genes out of this list were exressed in HeLa cells. In spite of the fact that many of those genes were shown to be targeted by HuR in different cell lines and often in stress conditions, 55 (81%) of the literature target genes were recovered in HuR PAR-CLIP, which is significantly more than expected by chance (p value < 2.7E-6 hypergeometric test).

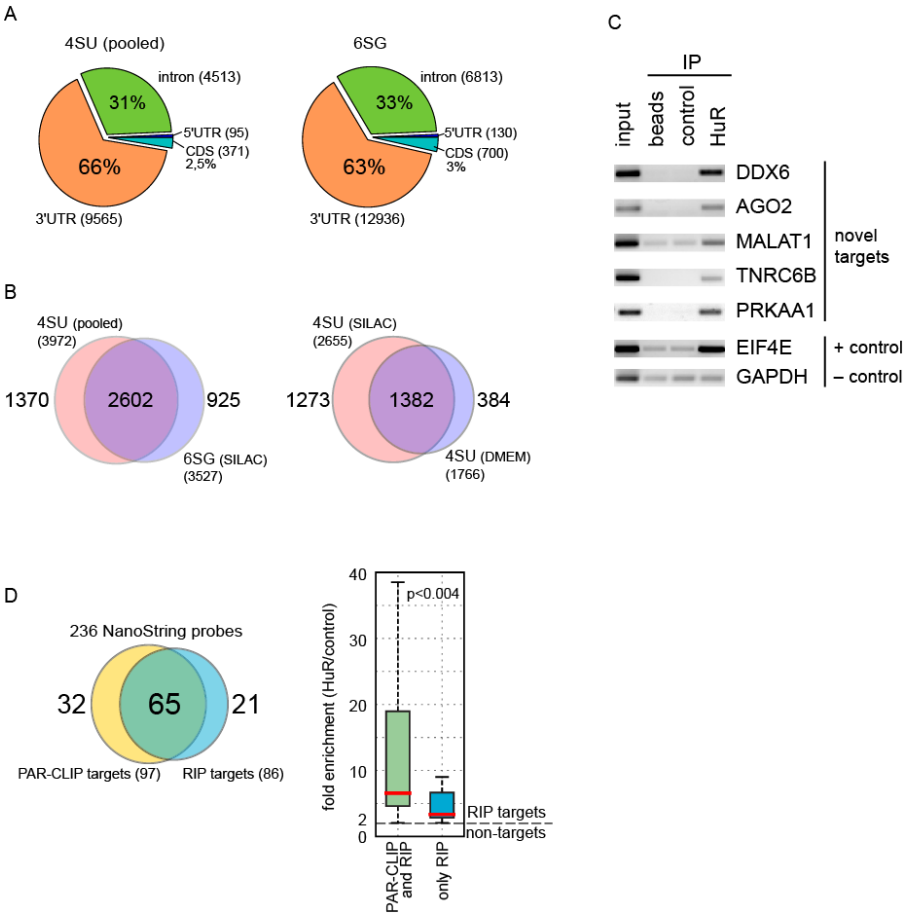

Figure 6. Reproducibility and validation of HuR PAR-CLIP

(A) The distribution of HuR clusters along transcripts (see Figure 5E) is reproduced if the clusters were called separately from 4SU or 6SG data. (The two 4SU libraries were pooled.) (B) (left) Target genes were independently called from pooled 4SU or 6SG experiments. 65%-74% of the target genes overlap between the two datasets. (right) Venn diagram of the overlap between target genes identified with 4SU PAR-CLIP in different media. (C) RIP and RT-PCR validation of HuR targets. IP without labeling or crosslinking was performed with anti-HuR antibody, anti-FLAG antibody as negative control or empty beads. 5/5 novel targets and the known target EIF4E were enriched in HuR pulldown, while the abundant GAPDH mRNA (negative control) was not. (D) Overlap between PAR-CLIP and RIP. mRNA from HuR IP was quantified on the Nanostring NCounter gene expression system. Genes enriched more than 2-fold over the control antibody were called RIP targets (blue). Out of 236 Nanostring probes, 97 genes belonged to the PAR-CLIP consensus target set (yellow). 65 of them overlapped with RIP targets (green). (E) Among RIP targets, those that were also identified by PAR-CLIP (green) had significantly higher enrichment in HuR pulldown than those that were not (blue).

To validate PAR-CLIP with an independent method, we performed a traditional RIP assay, which does not involve photoreactive nucleoside labeling or UV crosslinking. We confirmed co-immunoprecipitation with HuR for five PAR-CLIP HuR targets by RT-PCR (Figure 6C). To more systematically compare PAR-CLIP and RIP, we analyzed total RNA immunoprecipitated with anti-HuR and control anti-FLAG antibody on the Nanostring nCounter assay [108]. This medium-scale mRNA quantitation assay is based on counting single mRNA molecules hybridized to a chip with pre-designed probes and does not involve conversion of RNA to cDNA or PCR amplification. The Nanostring assay quantified 236 genes, out of which 97 belonged to the consensus target set ("PAR-CLIP targets" in Figure 6D). We called genes that were at least two-fold enriched in HuR IP over the FLAG IP in the RIP assay as "RIP targets" (86 genes out of 236). Out of the 86 RIP targets, 65 were also PAR-CLIP targets. The remaining 21 targets that were not identified as PAR-CLIP targets were called "RIP only" targets. We reasoned that they are likely to be indirect interactors. This assumption is supported by the fact that they were significantly less enriched in the HuR IP than the PAR-CLIP targets (Figure 6D, right).

3.3. PAR-CLIP recovers known HuR binding sequences.

HuR had been known to bind AU-rich sequences, but previous attempts to define a consensus binding motif were inconclusive, reporting either a hairpin [109] or a single-stranded U-rich motif [110]. Having the nucleotide resolution HuR binding data from PAR-CLIP, we were able to infer the sequence preference of HuR binding. We compared the abundance of all 7-mers in 41nt regions centered around crosslink sites that showed the most nucleotide conversions (crosslink centered regions, CCRs) in 4SU and 6SG PAR-CLIP clusters (Figure 7). We found a good agreement between 4SU and 6SG experiments (Spearman 0.88) again confirming PAR-CLIP reproducibility.

Indeed, U-rich motifs were predominant among HuR-bound sequences. The top three 7-mers enriched in 6SG PAR-CLIP, UUUUUUU, UUUAUUU and UUUGUUU, exactly corresponded in sequence and order to the highest rank HuR binding motifs derived from *in vitro* binding studies [111]. The classical AU-rich element (AUUUA) was also present as a part of several highly enriched AU-rich 7-mers. Interestingly, also CU-rich, but not GU-rich, motifs were highly enriched, in exonic as well as in intronic clusters, indicating that HuR possibly binds polypyrimidine tracts (see below).

We asked whether HuR binding sites had any specific secondary structure, since one of the previous studies reported a stem-loop sturcture as part of the HuR binding motif [109]. We calculated the base-pairing probability for windows of 201 nt around CCRs [107]. HuR sites had significantly less

base-pairing probability than the control regions randomly chosen in the same 3'UTR. We therefore concluded that HuR tends to bind single-stranded RNA. This is consistent with previous *in vitro* findings [111], as well as the crystal structure of the first two RRM domains of HuR [112] fitted

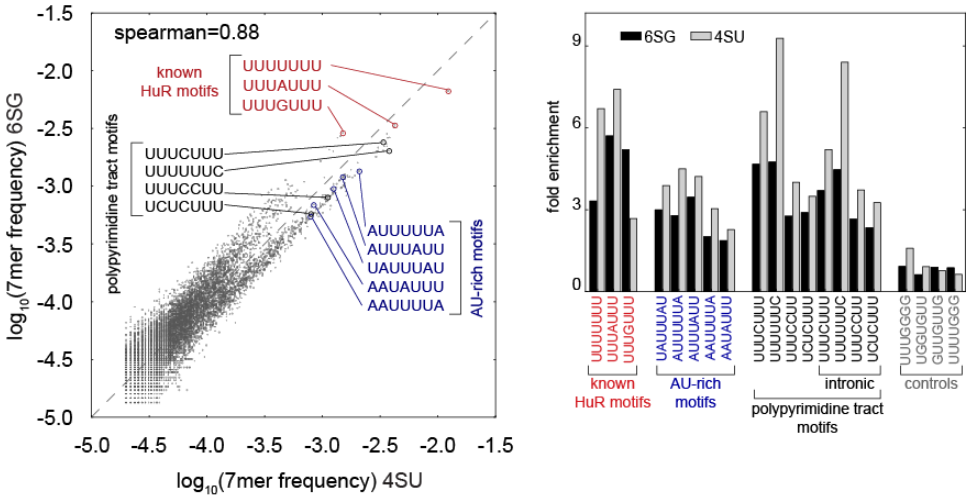

Figure 7. HuR binding motifs. *(left)* Correlation between 7-mer frequencies in the 6SG versus 4SU PAR-CLIP experiments. The most abundant 7-mers UUUUUUU, UUUAUUU, and UUUGUUU match known high affinity *in vitro* motifs [113]. AU-rich elements (AREs) and polypyrimidine motifs are also frequent. *(right)* Fold enrichment of the 7-mers in PAR-CLIP clusters compared to all human 3'UTRs. U-, AU- and pyrimidine-rich motifs are highly enriched. Control GU-rich 7-mers are not enriched despite of high content of the labeling nucleosides, 4SU and 6SG.

onto the known structure of the closely related HuD protein [113].

3.4. HuR interaction with miRNAs.

Since several cases of HuR interaction with miRNAs on the same 3'UTR were described, we used the HuR PAR-CLIP and available high throughput data on miRNA binding to investigate these interactions on a transcriptome-wide scale. First, we asked for the conservation pattern of the HuR binding sites and the surrounding context in the 3'UTRs. We plotted the average nucleotide conservation score of 201nt regions centered on the CCRs (Figure 8A, blue line). Control regions were randomly chosen in the same 3'UTR (black line). The ~6nt around the crosslink were highly conserved above background. Flanking areas also were singificantly more conserved than the

background, suggesting the presence of other conserved functional sequences in close proximity to the HuR binding sites.

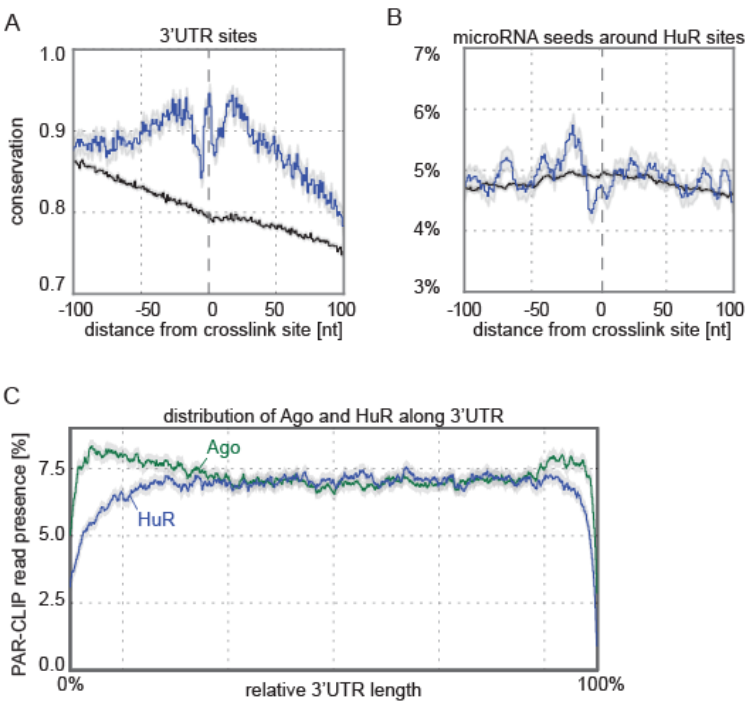

Figure 8. HuR and miRNA target sites in 3'UTR. (A) 3' UTR binding sites of HuR are highly conserved. HuR clusters were aligned at the position of the strongest crosslink (designated by 0 and later referred to as “anchor”) and the average PhyloP conservation score was plotted in a 201nt around the crosslink for HuR sites (blue) and control windows randomly chosen in the same 3'UTR (black). The grey envelope represents the stadard error of the mean. 3' UTR binding sites display a core of approximately six conserved nucleotides and flanking regions of high conservation, possibly indicating other regulatory elements. (B) miRNA seeds are proximal to but rarely overlap HuR sites. Density of predicted conserved miRNA seeds around anchors in 3'UTRs. HuR anchors and seeds display no tendency for direct overlap but the larger context (10–20 nt) shows an elevated seed density. (C) HuR and AGO binding profiles on 3'UTRs are different. AGO PAR-CLIP read presence peaks in the beginning and in the end of 3'UTRs. HuR appears to avoid proximity to coding sequences and close proximity to the site of polyadenylation.

We reasoned that one type of abundant conserved regulatory sequences in 3'UTRs contributing to this pattern could be miRNA target sites. We used both computational and experimental data to

assess if miRNA binding sites were specifically associated with HuR binding sites on a transcriptome-wide scale. First, we used computationally predicted miRNA target sites (predicted by the PicTar [9; 10] or TargetScan [11] algorithms). The density of the predicted conserved miRNA seeds in a 201nt window around the anchors is shown in Figure 8B. Less miRNA seeds directly overlap HuR sites (blue line) than in randomly selected regions of 3'UTR (black line). However, miRNA seeds were enriched in close proximity to HuR binding sites, consistent with the conservation pattern in Figure 8A.

We also used available binding data for human Ago1-4 from PAR-CLIP in HEK293 cells [13]. We contrasted the distribution of PAR-CLIP reads for Ago and HuR along all human 3'UTRs on a relative length scale (Figure 8C). Consistent with the previous reports, Ago preferentially binds in the beginning and in the end of 3'UTRs. On the contrary, HuR is uniformly distributed over 3'UTRs, rather avoiding areas close to the stop codon and the polyadenylation site.

To conclude, direct competition between HuR and RISC for the same binding site seems to be rather uncommon. Neverthless, it is not excluded, since ~700 HuR binding sites do overlap with miRNA seeds. The more general scenario seems to be binding of HuR and the RISC complex in close proximity in a non-overlapping fashion.

3.5. HuR knock down results in specific downregulation of HuR target mRNAs.

To test whether the large number of HuR interactions uncovered by PAR-CLIP were functional we asked how HuR targets behave upon change of HuR protein concentration. Since HuR is a known regulator of both mRNA stability and translation, we followed mRNA and protein levels as well as protein synthesis rates on the global scale after depletion of HuR.

We transfected HeLa cells with siRNA targeting HuR mRNA. We used two different siRNAs in parallel to account for likely off-target effects (see below). One technical limitation of the siRNA approach was that HuR has a very fast turnover mRNA (half-life time ~9h), however HuR protein is very stable (half-life time >85h in mouse) [3]. Moreover, HuR is an abundant protein (see discussion) and therefore a high efficiency of the knock down (at least 80% from our experience) was required to achieve appreciable response. However, an efficient siRNA knock down is technically difficult to achieve for fast turnover mRNAs which are more resistant to siRNA silencing [114]. Therefore, we performed a time course following the transcript abundance at 2 days (2d) and 5 days (5d) after siRNA transfection. Protein levels were measured at 5d post-transfection, and a pulse-labeling experiment quantified protein synthesis rates starting at 2.5d post-transfection.

We measured transcript abundances by sequencing poly(A) RNA on the Illumina Genome Analyzer.

Either 76 bp or 100 bp from both ends of the paired-end library were sequenced and mapped to th human genome using the TopHat mapper [115]. Technical and biological reproducibility of the RNA-Seq was high (Figure 9A,B). We also sought to validate RNA-Seq measurements with an independent method. We used the Nanostring NCounter Assay to quantify mRNA levels and compared Nanostring counts to transcript abundances inferred from RNA-Seq. Overall correlation was good (Figure 9C).

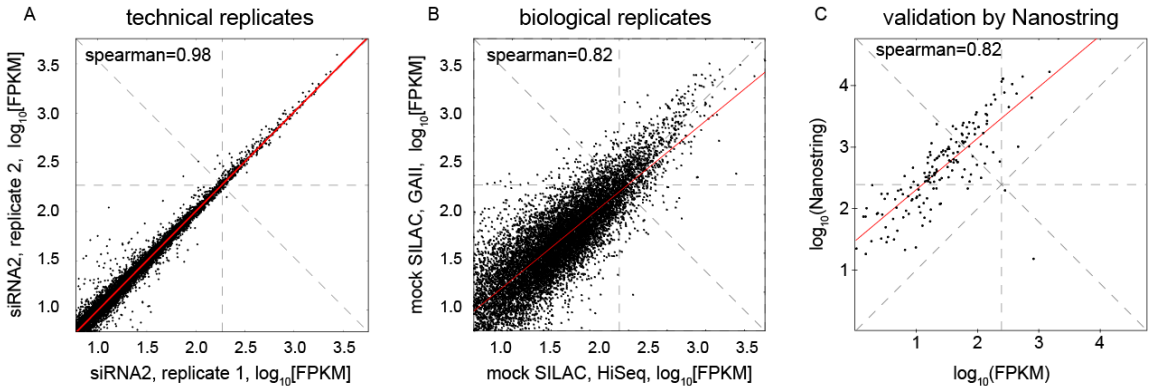

Figure 9. Technical and biological reproducibility of mRNA sequencing. (A) For technical replicates, RNA isolated from cell transfected with siRNA2 was divided in two parts, and poly(A) mRNA isolation and sequencing library preparation was done in parallel. (B) Biological replicates of mock-transfected cells grown in SILAC medium were sequenced using different generations of Illumina sequencing machines, Genome Analyzer (GAII) (2 x 76 bp paired-end sequencing) and newer generation HiSeq (2 x 100 bp). (C) Validation of mRNA sequencing by the Nanostring Ncounter assay. mRNA levels are shown as $\log_{10}$ of FPKM units (fragments of read pairs per kilobase of exon per 10^6 read pairs) or as $\log_{10}$ of Nanostring counts. Red lines show best fit.

We then compared fold changes in mRNA levels for HuR targets and non-targets. Consistent with the mRNA stabilizing role of HuR, upon HuR knock down transcript levels were significantly (p value ~ 0) more downregulated for HuR targets than for the non-targets (Figure 10). Moreover, the effect of downregulation correlated with the strength of HuR-target interaction, as the top 20% highest ranking targets (sorted by the number of HuR binding sites) showed stronger down regulation (pink line in Figure 10). Traditionally, the role of HuR in mRNA stability was thought to be mediated solely by the 3'UTR. We therefore checked whether the levels of intronic HuR targets were affected by HuR knock down. Indeed, intronic targets were significantly downregulated (blue dashed line in Figure 10), confirming functionality of intronic HuR interactions.

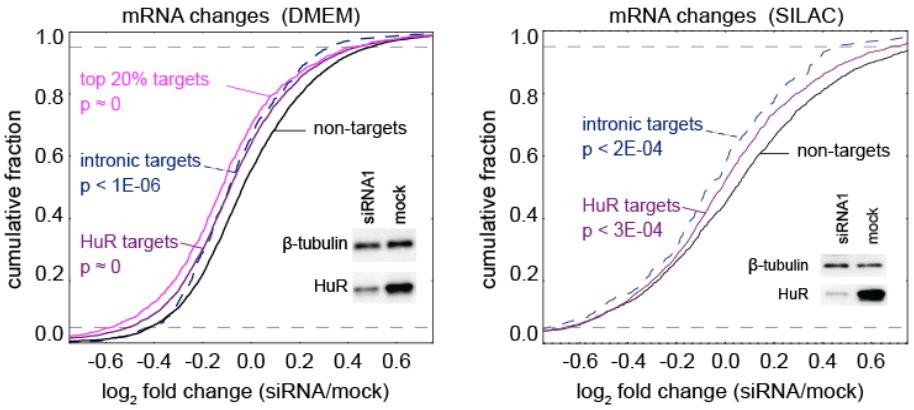

Figure 10. HuR target mRNAs are destabilized upon knock down of HuR. Cumulativ density fractions of mRNA log2 fold changes. For each number corresponding to a fold change (shown as log2 of the ratio of FPKM in siRNA-transfected cells and mock transfected cells) the curve shows the fraction of genes with the foldchange less or equal to that number. P values show the result of a t-test on the foldchange distributions. HuR targets are destabilized upon knock down of HuR. Targets with most binding sites (pink) show the strongest effect both in DMEM (left) and SILAC medium (right). Genes with exclusively intronic binding of HuR (dashed line) are also highly significantly down regulated. Inserts show Western blot validations of the HuR knock down.

SiRNA knock down experiments are prone to off-target effects, when the siRNA acts as a miRNA and downregulates genes that have "seed" complementary sequences in their 3'UTRs. We performed an unbiased search for sequence motifs significantly associated with up- or downregulation in our data (see supplementary material [107]) with the miReduce algorithm [116]. SiRNA seed sequences were indeed significantly associated with downregulation. Since HuR targets have on average longer 3'UTRs (supplementary material [107]), they are also more likely to contain sequences complementary to the siRNA used for the knock down. Thus, HuR targets might be more affected by siRNA off-targeting than the non-targets. To rule out this possibility, we repeated the analysis with all mRNAs containing the siRNA seeds removed. It should be noted that this procedure eliminates a large part of HuR targets from the analyzed mRNA pool, because they are more likely to bear siRNA seeds than the non-targets. In spite of that, downregulation of HuR targets was still significant ($p < 1E-02$). As an additional test, we only considered genes that had consistent changes in both siRNA experiments, enriching for direct HuR effect, and also observed significant downregulation of HuR targets compared to non-targets ($p < 1E-04$, [107]).

3.6. HuR knock down specifically decreases protein synthesis of target genes.

Although many RBPs are known that regulate translation of their target mRNAs, no study to our knowledge has investigated the global effect of an RBP on translation. We measured the effect of HuR depletion on protein steady-state levels and protein synthesis rates, using SILAC (Stable Isotope Labeling with Amino acids in Cell culture) based quantitative mass-spectrometry [117]. The SILAC method accurately quantifies thousands of protein fold changes between two differentially treated samples (Figure 11).

To measure the effect of HuR on global protein synthesis, we used a modification of the SILAC method called 'pSILAC' (pulsed SILAC) [31]. In pSILAC, essential amino acids arginine and lysine, containing heavy isotopes, are incorporated into newly synthesized proteins during a short (24h) pulse labeling. Two different mass labels, “heavy”(H) and “medium-heavy”(M) are used for the control and HuR knock down, respectively. In the resulting mass spectrum, the mass shift between differentially labeled peptides allows to quantify changes in newly synthesized protein while the preexisting proteins are unlabeled (“light” [L]) (Figure 11). We were able to quantify ~ 4300 fold changes in protein synthesis. HuR targets were specifically and significantly downregulated compared to non-targets (Figure 11), consistent with the changes of the mRNA levels (Figure 10).

Quantifying steady state protein levels (Figure 11) requires close to complete labeling of proteins in SILAC medium (for at least 5 cycles of cell doubling, B. Schwanhäusser, personal communication). We chose a 5 days time point as a compromise between sufficient labeling time and still efficient HuR knock down. Surprisingly, steady-state protein levels for HuR targets as a group were not specifically downregulated as compared to non-targets (Figure 11). Interestingly, intronic targets of HuR were significantly downregulated at the steady-state protein levels (Figure 11). Several explanations of this effect and of differential behavior of intronic targets are possible (see discussion).

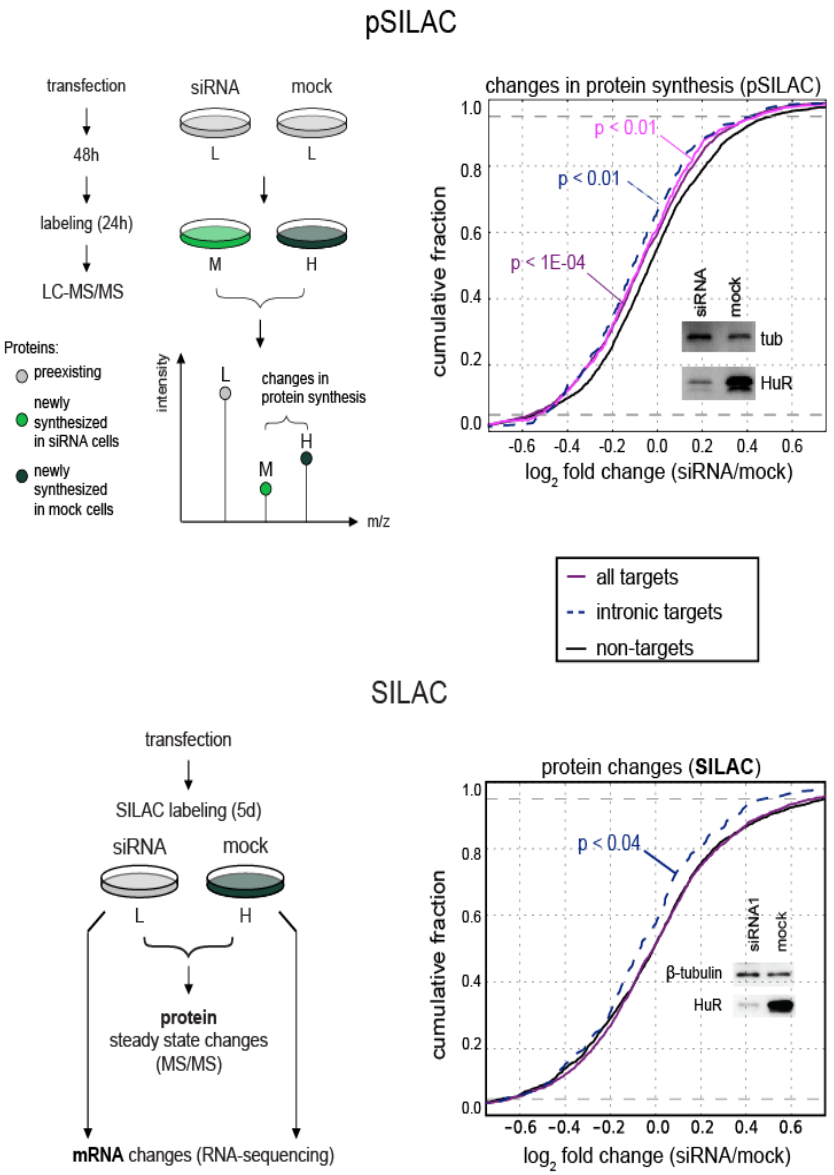

Figure 11. Effects of HuR knock down on protein synthesis and steady-state levels.

pSILAC measures changes in protein synthesis. (left) Principle of the method. Newly synthesized proteins incorporate heavy (mock) and medium-heavy (HuR knock down) amino acids on special medium for 24 hr. The mass shift allows measurement of the difference in newly synthesized protein between normal and HuR depleted cells, with LC-MS/MS (liquid chromatogaphy coupled to tandem mass spectrometry). (right) Protein synthesis of HuR targets is reduced upon HuR knock down. Cumulative density fractions of protein synthesis log2 fold changes. Exonic(solid purple line) and intronic (dashed blue line) targets of HuR are significantly downregulated after knock down. **SILAC** measured protein steady state changes after HuR knock down. (left) Outline of the experiment. After siRNA (mock) transfection cells are grown in medium with light (heavy) amino acids. After 5 days proteins and mRNAs are extracted. Changes in protein steady state levels are measured by mass spectrometry, changes in mRNA levels by polyA(+) RNA sequencing. (right) CDF plot of log fold changes of steady state protein levels. "Intronic only" targets show significant downregulation. CDF plot of log fold changes of mRNA levels measured in the same sample as the protein changes is shown in Figure 10, right panel. Insert: Western blot validation of HuR knock down.

3.7. HuR-dependent changes in splicing.

Although ~90% of HuR is localized in the nucleus in unperturbed cells, intronic binding was not reported for HuR before. We found that ~1/3 HuR binding sites are located in introns. We asked if those sites reflected a background binding due to high abundance of HuR in the nucleus or played a possible functional role in mRNA metabolism. Sequence conservation is an indication of functionality, and we analyzed the conservation of intronic binding sites in the same manner as we did for the 3'UTR sites (see above). Intronic HuR binding sites were more conserved than the average intronic background (Figure 12A).

We next asked how HuR binding sites were distributed within introns. We looked at the PAR-CLIP read distribution along the relative intron length (Figure 12B). There was a prominent increase of

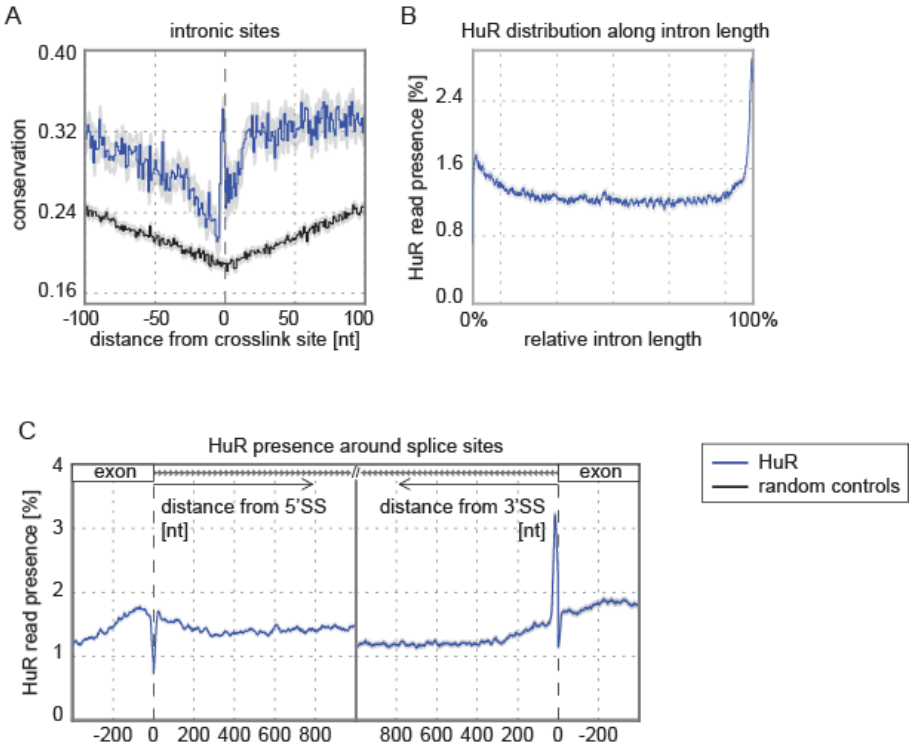

Figure 12. Intronic HuR binding sites are conserved and associated with splice sites.

(A) HuR inding sites in introns are conserved. HuR clusters were aligned at position of the strongest crosslink (0) and the average PhyloP conservation score was plotted in a 201nt around the crosslink for HuR sites (blue) and random control windows randomly chosen in the same intron (black). The grey envelope represents the standard error of the mean. (B) HuR is preferrebly binding close to splice sites. The plot shows the distribution of HuR binding (PAR-CLIP read density) along intron length on the relative scale from 0 to 100%. (C) HuR binding distribution plotted for an asymmetric window around splice sites. The peak of HuR binding is ~20nt upstream of the 3' splice site.

HuR binding towards splice sites, especially 3' splice site. A more detailed view of splice sites at nucleotide resolution revealed preferential HuR binding around 20-50nt upstream of 3' splice sites, which is predicted to overlap the polypyrimidine tract of most mammalian introns (Figure 12C). Together, these data suggested that HuR may be involved in the regulation of splicing.

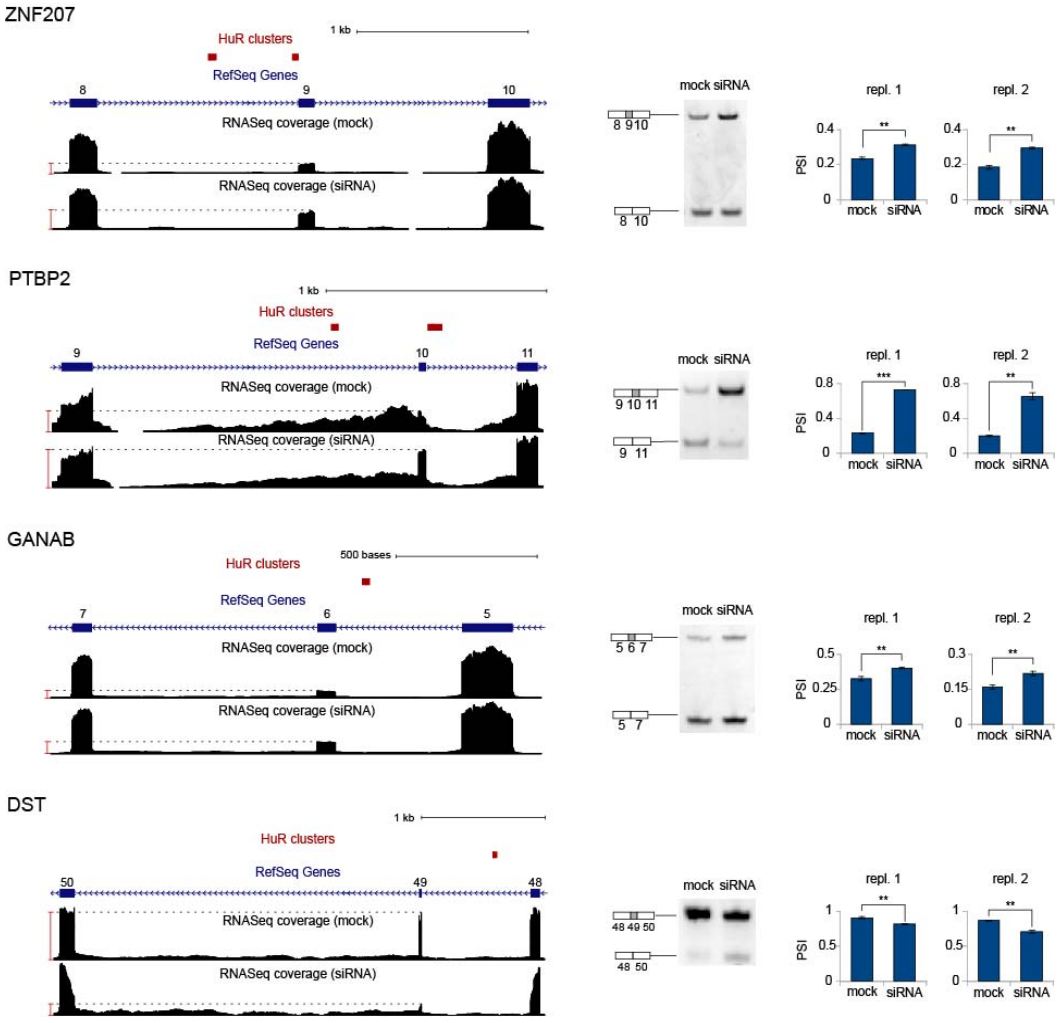

Figure 13. Splicing of alternative exons is affected by HuR. Shown are genomic loci centered on alternative exons flanked by constitutive exons. HuR binding sites are shown as red rectangles. Coverage profiles of RNA-Seq for mock-transfected and HuR-transfected cells are shown below.(right) Differential inclusion of alternative exons was validated by PCR with primers to the flanking exons. The PSI (Percent Spliced In) value was calculated from molar ratios of the PCR products quantified by Bioanalyzer.

We therefore searched in our HuR perturbation data for evidence of alternative splicing regulated by

HuR. The candidate HuR-dependent alternative exons should 1) bear at least one HuR binding site within 1 kb of the exon or in the exon itself; 2) change their inclusion ratio upon HuR knock down (we estimated exon inclusion from RNA-Seq data). We found 51 such exons, 21 were upregulated and 30 downregulated upon HuR knock down. We quantified the PSI (Percent Spliced In) ratio for 6 candidate exons with PCR and Bioanalyzer and validated the splicing change for 4 out of 6 in two independent biological replicates (Figure 13).

The most prominent AS change observed was the increase of inclusion of exon 10 of PTBP2 gene from ~20% in unperturbed conditions to 70% upon depletion of HuR (Figure 13). Exon 10 is flanked by two HuR binding sites. PTBP2 is a neuron-specific paralog of PTBP (polypyrimidine tract binding proteins). In non-neuronal tissues, exon 10 is skipped and this leads to nonsense-mediated decay (NMD) of PTBP2 mRNA. Indeed, after HuR knock down, PTBP2 protein synthesis was upregulated >4 fold, while the mRNA was up only 1.2 fold, strongly suggesting that HuR is involved in tissue-specific post-transcriptional regulation of PTBP2 expression.

3.8. HuR regulates miR-7 processing.

Several RBPs regulate miRNA processing [59; 60; 118]. To assess the effect of HuR on mature miRNA levels, we analyzed small RNAs from unperturbed and HuR-depleted HeLa cells (Figure 14). Strikingly, miR-7 was strongly and specifically upregulated while other miRNAs almost did not change. MiR-7 was upregulated ~20-fold when HuR was knocked down with siRNA1 and ~5-fold with the less efficient siRNA2 (Figure 14B). Despite low levels in unperturbed HeLa cells, miR-7 is readily detectable by Northern blotting and qPCR, and these experiments confirmed upregulation of miR-7 (Figure 14B,C). Consistently, upon over expression of GFP-tagged HuR a reduction of mature miR-7 over expression was observed (Figure 14C).

MiR-7 can potentially originate from three loci in the human genome. We could exclude two by analyzing deep sequencing reads corresponding to the star and precursor sequences. We used the miRDeep2 [8] algorithm to look at the distribution of the sequencing reads for the three miR-7 precursors in the human genome. ~160 reads mapping to the star, loop and flanking regions could be explained by miR-7-1, but not by miR-7-2 or miR-7-3. In addition, there was no evidence for expression of miR-7-2 and miR-7-3 in our RNA sequencing data. Therefore, miR-7-1 is likely the only source of mature miR-7 in HeLa cells. MiR-7-1 is situated in the last intron of the highly expressed housekeeping gene HNRNPK (Figure 14D). This intron and the flanking exons bear multiple strong HuR binding sites, and HNRNPK exression level does not change upon HuR knock down. In sum, this suggests that miR-7 levels could be directly regulated by HuR at the level of the

precursor processing.

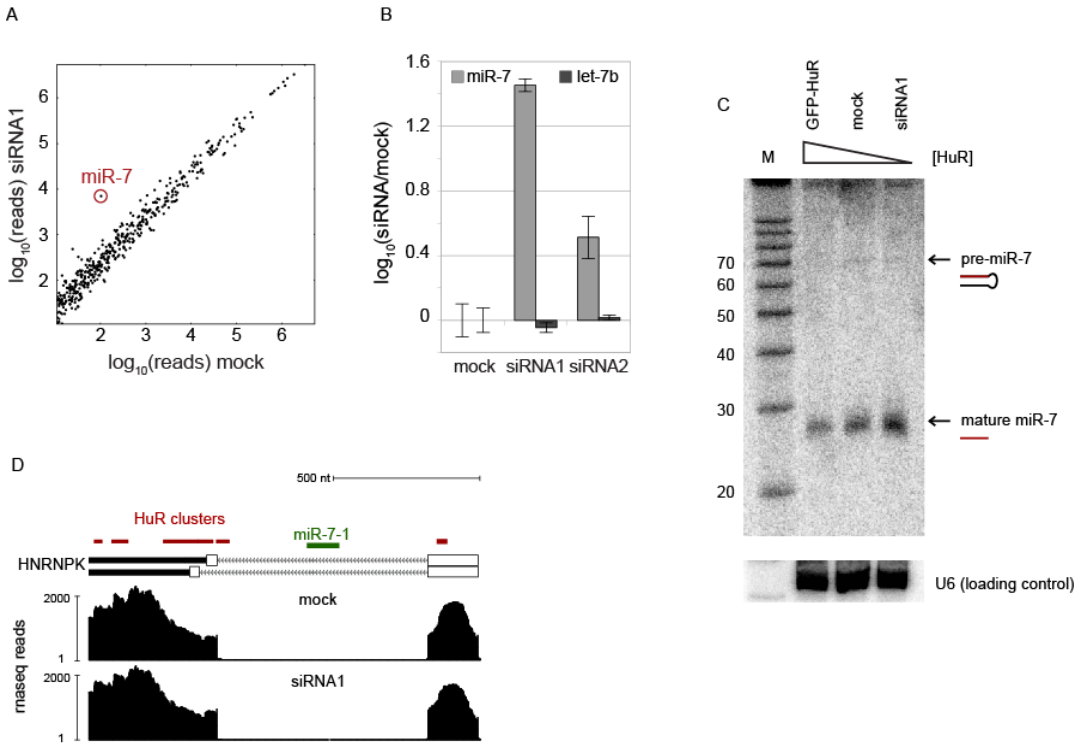

Figure 14. Suppression of miR-7 biogenesis correlates with HuR expression. (A) Mature miRNA expression upon HuR knock down. Plotted are log10 of read counts corresponding to mature miRNAs for mock- and siRNA1-transfected cells. Mature miR-7 was the strongest upregulated miRNA upon knock down of HuR. (B) Validation of miR-7 upregulation by qPCR. Mature miR-7, but not abundant let-7b, showed dose-dependent upregulation upon knock down of HuR (siRNA1 is more efficient than siRNA2). Endogenous control was U6 snRNA. Error bars indicate 95% confidence interval. (C) Validation of miR-7 regulation by Northern blotting. Mature miR-7 is upregulated upon HuR knock down and downregulated upon over expression of GFP-tagged HuR. (D) HuR directly binds to the last intron of HNRNPK that harbors miR-7-1 precursor and to the flanking exons. Two alternative splicing isoforms of HNRNPK are shown. Red boxes indicate HuR binding sites, the green box indicates the miR-7-1 precursor. The RNA sequencing profile shows that high expression of HNRNPK and its splicing pattern are independent of HuR knock down.

3.9. HuR targets are involved in post-transcriptional regulation.

We performed a gene ontology (GO) term analysis of HuR target genes. “mRNA metabolic process”, “RNA splicing” and “mRNA processing” were the most prominent enriched GO term

categories among HuR targets (Table 2). Genes in these categories included components of the spliceosome (snRNPs and auxiliary splicing factors), the mRNA degradation machinery (subunits of the CCR-NOT deadenylase complex, exosome and decapping complex, as well as miRNA effectors TNRC6 and AGO2), and multiple RNA-binding proteins (PABP, QKI, IGF2BP1, proteins of RBM and HNRNP families and HuR itself). This is consistent with mutual auto- and cross-regulation of post-transcriptional regulators and argues for HuR being one of the hubs of the regulation of RNA metabolism.

HuR is known to regulate cell cycle genes [96] and beta-actin mRNA [82] , and consequently, “Cell cycle”and “cytoskeleton organization” are among the top enriched GO terms. In addition, “Regulation of transcription” and protein degradation (“protein ubiquitination” and “cellular protein catabolic process”) link the post-transcriptional regulator HuR to transcriptional and post-translational regulation.

Table 2: Enriched GO terms among HuR target genes (for the full list of GO terms, see [107], online supplementary material).

GO Term (Biological Process)	Count	Fold Enrichment	P-value (Benjamini)	FDR
GO:0016071~mRNA metabolic process	129	2.3	1.70E-17	7.65E-018
GO:0006397~mRNA processing	109	2.2	1.03E-13	9.25E-014
GO:0045449~regulation of transcription	537	1.4	1.53E-13	2.11E-013
GO:0008380~RNA splicing	96	2.2	5.89E-012	1.59E-011
GO:0007049~cell cycle	198	1.7	1.04E-011	4.20E-011
GO:0008104~protein localization	218	1.6	1.38E-011	6.23E-011
GO:0044257~cellular protein catabolic process	161	1.8	4.17E-011	2.82E-010
GO:0010608~posttranscriptional regulation of gene expression	68	2.1	9.41E-008	1.82E-006
GO:0007010~cytoskeleton organization	111	1.7	1.80E-006	4.23E-005
GO:0016567~protein ubiquitination	43	2.4	3.53E-006	8.75E-005

3.10. HuR/ELAVL1 has a role in vascular development in zebrafish.

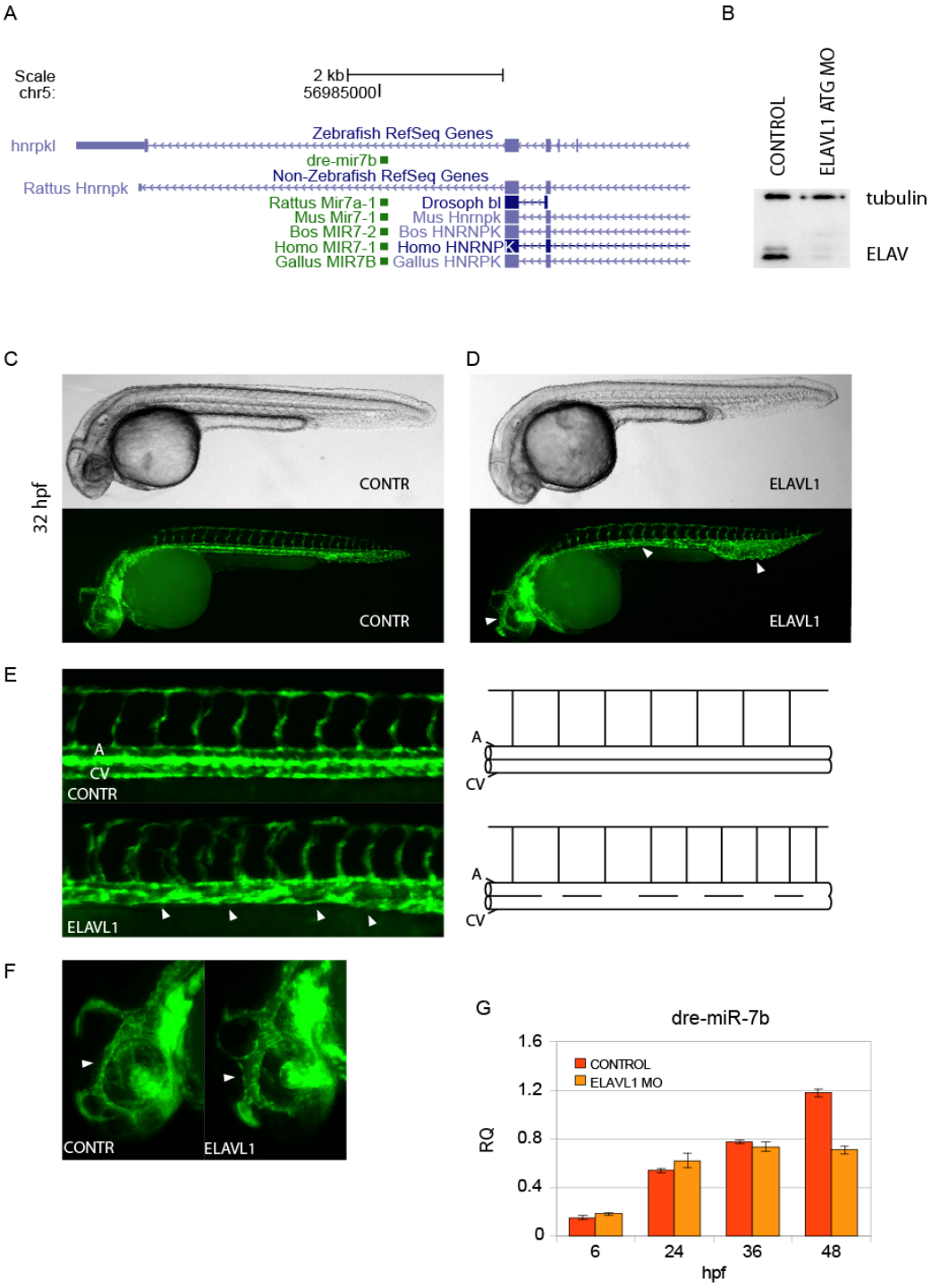

Figure 15. ELAVL1 depletion in zebrafish causes vascular development defects. (A) miR-7 precursor localization to the last intron of HNRNPK gene is conserved among vertebrates and in Drosophila. UCSC genome browser screenshot shows the alignment of the homologs of the HNRNPK gene and pre-miR-7. (B) Embryos of Fli:eGFP transgenic line were injected with the standard control morpholino (MO) and the MO against ELAVL1. Western blot validation of the ELAVL1 protein knockdown at 24hpf. ►

► (C, D) Control embryos (C) and ELAVL1 morphants (D) were imaged at 32hpf (hours post fertilization). Shown are light microscopy images (above) and the corresponding GFP images (below) at 50x magnification. Fli:eGFP marks the endothelial cells. ELAVL1 morphants show fusions in eye vessels, in the trunk and in the caudal vein plexus (arrowheads).(E) Trunk vessels at 100x magnification (left) and their schematic representation (right). While the aorta (A) and the caudal vein (CV) are clearly separated in control animals, ELAVL1 morphants show multiple shunts between the aorta and the vein (arrowheads). (F) Head vessels at 100x magnification. ELAVL1 morphants (right) show fusion of eye vessels compared to control (arrowheads). (G) TaqMan real-time PCR quantification of dre-miR-7b expression during the first 48h of development in control embryos and ELAVL1 morphants.

We were further interested to investigate whether miR-7 processing could be regulated by HuR *in vivo*. The localization of the miR-7 precursor to the last intron of the HNRNPK gene is conserved in vertebrates and even in *Drosophila* (Figure 15A). Moreover, in these organisms mature miR-7 expression is restricted to a few neurosecretory tissues [119] [120] [121] whereas its primary transcript, HNRNPK, is ubiquitously and highly expressed. Given the as well high conservation and ubiquitous expression of the HuR/ELAVL1 protein in these organisms, we hypothesized that HuR might block ectopic production of miR-7 in the majority of the tissues.

We decided to test this hypothesis in zebrafish. We chose this model organism because its development is fast, the embryos are easy to inject with antisense oligonucleotides, and the transparency of embryos and availability of GFP reporter lines allows screening for possible phenotypes.

In zebrafish, the *miR-7b* is located to the last intron of the *hnrnpkl* gene (Figure 15A). We designed an antisense morpholino (MO) oligomer targeting the translation start site of the *Danio rerio* ELAVL1 mRNA. The ELAVL1 protein was efficiently downregulated in the injected embryos (Figure 15B). We then profiled the miR-7b expression in the course of the first 48h of development (Figure 15G). Mature miR-7b expression is already detectable at 24 hpf (hours post fertilization). However, no significant difference between control embryos and ELAVL1 morphants was observed. The downregulation of miR-7b in the ELAVL1 morphants at 48 hpf might be a secondary effect, since these morphants show clear defects in development (see below).

For our experiments we used a Fli:eGFP reporter zebrafish line which expresses GFP in endothelial cells and allows monitoring of the vascular system development. We observed severe defects in the developing vessels of the ELAVL1 morphants compared to the controls (Figure 15C,D). In particular, the ELAVL1 morphants showed artery-vein differentiation defects, reflected in an incomplete separation of the aorta from the caudal vein(Figure 15E). Brain vessel defects were also

observed (Figure 15F). Together, this is consistent with the fact that the key vessel growth regulators HIF1A and VEGF are known targets of ELAVL1 in mammals, and are confirmed to be strong HuR targets by our PAR-CLIP assay. We are currently investigating whether other miRNAs are misregulated in ELAVL1 morphants and whether misregulation of their target mRNAs could explain the observed phenotype.

4. Discussion

4.1. HuR regulates thousands of target genes in human cells.

We report almost 5000 functional target genes of HuR in HeLa cells. Overall HeLa cells express about 11000 genes, thus HuR binds almost half of the HeLa cell transcriptome. This number is consistent with the fact that HuR is a highly abundant protein (in a recent study [3] which quantified absolute protein numbers in mouse NIH3T3 cells, HuR was in the top 6% most abundant proteins with ~5E+05 molecules/cell). Together with the notion that HuR is ubiquitously expressed, this implies that HuR could play a general role as a core component of many mRNPs. Since HuR is very abundant in the nucleus, and we report numerous intronic binding sites, HuR is likely to take part in pre-mRNA processing. This is reinforced by the fact that HuR was found to associate both with pre-mRNA hnRNPs in the nucleus and mature mRNPs in the cytoplasm [122] . Since HuR actively shuttles between nucleus and cytoplasm [123], these data argue for a possible role of HuR in mRNP transport.

4.2. Comparison of RIP and PAR-CLIP.

The advantages and drawbacks of CLIP and RIP methods have been discussed above. We showed that the targets which are common to RIP and PAR-CLIP are likely to be the strongest and direct targets compared to those only enriched in RIP. Notably, another study co-submitted with ours [124] has made a similar comparison between PAR-CLIP and RIP targets of HuR. Mukherjee et al. report a similar degree of overlap between PAR-CLIP and RIP targets. Complementing our results, the authors compared “PAR-CLIP and RIP” targets to “PAR-CLIP only” targets and showed that the latter had less HuR binding sites than the targets reported by both RIP and PAR-CLIP [124]. In conclusion, mRNA targets identified by both PAR-CLIP and RIP are enriched for stable interactors. Additionally, PAR-CLIP identified transient interactions of HuR because of the high crosslinking efficiency.

4.3. HuR binding motifs.

We used both 4SU and 6SG labels to avoid a sequence dependent bias in PAR-CLIP. Although the overall correlation between the two labels was high, the UUUGUUU motif was slightly less enriched in the 4SU PAR-CLIP. The reason for this could be the usage of RNaseT1 which cleaves RNA after G. While our manuscript was in preparation, another group [125] has thoroughly investigated the connection between RNase T1 digestion time and the degree of loss of G-containing sequences in the PAR-CLIP results, on the example of PAR-CLIP of HuR. The authors showed that overdigestion with RNase T1 may lead to specific depletion of G-containing sequences. Thus, carefully limiting digestion with RNase T1 in our experiments was crucial to avoid depletion of G-containing sequences.

Polypyrimidine sequences were frequent among HuR-bound 7-mers, and HuR binding in introns was concentrated in polypyrimidine tracts. This fact points to a possible competition of HuR with other polypyrimidine tract binding proteins, such as PTB or the general splicing factor U2AF. Given the abundance of HuR in the nucleus, it would be interesting to obtain PAR-CLIP data of U2AF and HuR under different concentrations of HuR in the cell (HuR knock down and over expression).

We observed that HuR binds a wide spectrum of U-containing sequences, which does not only include AREs, but also UC-rich and G-containing motifs. The lack of a strong consensus binding motif is not unique to HuR. Multiple RBPs recognize low complexity motifs, and RBPs with strictly defined consensus sequence (such as Pumilio) are rather rare [12]. It is tempting to speculate that many RBPs may play a buffering role, and for most of their targets a strong effect of the RBP depletion is not expected. This could probably explain the relatively small magnitude of gene fold changes that we observed both on mRNA and protein levels upon knock down of HuR.

4.4. Effects of HuR on protein levels

We did not observe specific downregulation in target protein steady-state levels at the late time point (5d) of the HuR knock down, with the exception of the intronic targets. Several explanations of this effect are possible. At the late time point of the knock down indirect compensatory effects possibly contribute to returning the system to the initial state (despite the fact that HuR downregulation was stronger at 5d than at 2d time point). This is consistent with our observation that mRNA levels return to the unperturbed state at 5d post-transfection in DMEM (not shown). Another possible explanation would be slow protein turnover specifically of HuR 3'UTR targets, but not of the intronic targets. We estimated protein turnover rates using our pSILAC data [107] and found that indeed, intronic targets were turning over significantly (p value ~ 0) faster than the

exonic targets. Thus, for 3'UTR targets, the constant steady state protein levels do not contradict the observed changes in protein synthesis. For intronic targets with fast protein turnover, both reduced protein synthesis rate and steady-state levels could be detected.

Interestingly, for intronic targets, mRNA changes were the least correlated with corresponding protein changes, while for 3'UTR targets the correlation was higher (not shown). This suggests that 3'UTR targets are regulated at the mRNA stability level, and changes in protein synthesis mostly reflect changes of mRNA. On the contrary, for intronic targets, mRNA changes are decoupled from changes in protein synthesis. This builds up evidence for a role of HuR in the pre-mRNA processing of its intronic targets.

To complement changes in protein synthesis rates, a meaningful experiment would have been the quantitation of changes of mRNA half-lives upon knock down of HuR (this can be done using pulse labeling with 4-thiouridine [126]). However, mRNAs have one order of magnitude faster turnover rates than proteins [3], therefore steady-state mRNA levels generally reflect the changes of mRNA stability.

4.5. HuR binding sites are conserved and located in proximity to other regulatory elements

We showed that both 3'UTR and intronic HuR binding sites are not only themselves conserved, but are often situated in a context of highly conserved sequence. This suggests a possible interaction of HuR with other post-transcriptional regulators when they bind next to each other on the same transcript. In 3'UTRs, miRNA seeds may be a part of the elements associated with HuR. Direct competition between HuR and miRNAs seems rare, but closely spaced arrangement of the RISC complex and HuR protein seems to be preferred, in agreement with the previously reported AU-rich sequence context for functional miRNA seeds [127].

Intronic HuR binding sites tend to be close to splice sites, and the proximity of exons can explain the broad areas of elevated conservation flanking intronic sites. Approximately the same number of alternative exons were included or excluded upon HuR knock down, and there was no one-to-one correspondence between HuR binding site position relative to the exon and the exclusion/inclusion pattern of the exon. This suggests complex alternative splicing rules, where HuR plays the role of an auxiliary regulator rather than a master splicing regulator of its targets (an example of such “master regulators” are Nova proteins in the brain). Each alternative exon inclusion rate is a result of a combination of splicing regulators binding to it and nearby, and it is not straightforward to predict changes in splicing after removing only one of the RBPs.

4.6. Regulation of PTBP2 by alternative splicing

PTBP2 exon 10 showed the most prominent change of inclusion rate upon knock down of HuR. One of the two flanking HuR binding sites is situated immediately downstream of exon 10 and coincides with U1 snRNP binding on the 5' splice site. Thus HuR binding may inhibit splicing of this exon. We constructed a splicing minigene reporter containing PTBP2 exon 10 and the two flanking exons. Mutating the 5'SS HuR binding site in the minigene construct partially impaired exon 10 inclusion, confirming functionality of this site (not shown). However, the HuR dependency of exon 10 splicing change was not eliminated by the introduced mutations, thus the influence of the second binding site is unclear.

PTBP2 is a neuron-specific paralogue of the ubiquitously expressed PTBP1. These two proteins supress each other by cross regulating alternative splicing, thus ensuring mutually exclusive expression patterns. PTBP2 exon 10 skipping was shown to be promoted by binding of PTBP1 on the 3'SS upstream of the exon 10 (a different site from the one bound by HuR) [128]. We ensured that the effect of HuR on PTBP2 was not mediated by PTBP1. HuR binds the 3'UTR of PTBP1, which is mildly destabilized (~20% downregulated on both mRNA and protein level) upon HuR knock down. However, it is not enough to explain the dramatic switch of the PTBP2 splicing pattern by this modest change PTBP1 alone. Moreover, HuR is lowly expressed in neuronal tissues, which is consistent with high expression of PTBP2. In sum, HuR and PTBP1 act together to ensure tissue-specific PTBP2 expression. Our findings place HuR among nuclear RBPs that affect alternative splicing, which already include the HuR homolog ELAV in Drosophila [129; 130] and human Hu/ELAV paralogs in neurons [65].

4.7. HuR regulates miR-7 processing

Processing of a miRNA can potentially be regulated at several steps. For intronic miRNAs, these steps are: 1) splicing of the host intron 2) Drosha cleavage 3) export of the pre-miRNA 4) Dicer cleavage. If miR-7 processing was regulated at the level of precursor export or Dicer cleavage, this would lead to accumulation of the unprocessed pre-miR-7. However, no accumulation of pre-miR-7 could be seen on the Northern blot (Figure 14C). Testing whether the Drosha processing step was affected by HuR would require to block Dicer and monitor the level of the pre-miR-7. However, extensive cell lethality upon double knock down of Dicer and HuR prevented us from performing this test.

The splicing factor SF2/ASF has already been shown to enhance miR-7 processing [61]. The miR-7 host gene HNRNPK has two alternatively spliced isoforms (Figure 14D). The splicing ratio of the

two isoforms did not change upon perturbation of HuR (not shown), consistent with the notion in [73] that the regulation of miR-7 processing is independent of the host gene splicing.

HNRNPK is highly and ubiquitously expressed, whereas miR-7 expression is restricted to a few neurosecretory tissues [121]. This argues for a requirement to decouple miRNA expression from expression of the host gene. HuR is a good candidate for performing this task, since it is highly and ubiquitously expressed and could contribute to preventing ectopic miR-7 expression in most tissues. We attempted to test this intriguing possibility in an *in vivo* zebrafish model. Although miR-7 was not downregulated in the preliminary qPCR assay, we are currently further investigating possible miRNA regulation by HuR/ELAVL1.

5. Conclusion and Outlook

In the last few years the rapid development of sequencing technologies allowed an unprecedented boost of the systems biology approaches to biological problems. On the one hand, this has rendered the use of bioinformatics crucial for projects involving high-throughput technologies. The lab of Nikolaus Rajewsky where I performed my work has been organized to maximize the interaction between bioinformaticians and experimentalists. All projects in the lab, including my own, described in the present thesis, are in essence a collaboration between a bioinformatician and an experimentalist, which involves discussions on a day-to-day basis.

On the other hand, the genomic, transcriptomic and proteomic view on cells and organisms led to new, unexpected questions. The discovery that most of the genome is transcribed raised the question about the role of non-coding RNAs, which is only beginning to be answered. Many classes of short and long non-coding RNAs are being described and sequence profiling can reveal their expression dynamics in different tissues and developmental stages. However, the functional analysis of their biological role and mechanisms of action is lagging behind. Specifically, deep sequencing boosted studies of small regulatory RNAs and showed that thousands of the cellular transcripts are regulated by them [31; 131] . Likewise, several studies of RBPs including our own showed the regulation of thousands of transcripts by RBPs. Despite the notion that RNA-binding proteins and microRNAs often have hundreds of targets, for most of the targets a destabilization (or stabilization) effect upon removal or overexpression of the RBP or microRNA is relatively mild (most of the changes lie within the range of 2-fold). Naturally, a concern arises whether all of the identified interactions are indeed functional, or, perhaps, the sequencing depth has become high enough to equally well detect transient interactions. We will need a means to distinguish which of the multitude of the identified interactions are functional, as, for example, subcellular-resolution and single-molecule experiments. On the other hand, the large number of interactions could reflect extensive redundancy among post-transcriptional regulators, consistent with an observation that one mRNA often bears binding sites for multiple miRNAs and RNA-binding proteins. Notably, while many genes prove non-essential for the survival of the organism in laboratory conditions, environmental challenge may reveal their function. Survival in stress conditions, in particular, requires a fast response and is likely to be regulated post-transcriptionally. Further experiments with changing conditions could reveal stronger responses of more specific targets.

In conclusion, accumulating high-throughput data on RBP and miRNA target interactions now need to be consolidated into a single post-transcriptional regulatory network with spatial and temporal information. This would provide a resource for hypotheses formation and testing. A quantitative

approach, integrating data about affinities of RBPs and half-lives of target mRNAs, needs to be obtained and integrated into the model. This map of the RNA interactome will help to define rules for post-transcriptional regulation by competition and/or combinatorial binding.

6. Materials and Methods

6.1. Cell culture and media

HeLa cells (CCL-2, ATCC) were cultivated at 37°C with 5% CO_2 in high glucose DMEM (Gibco, 41965), supplemented with 10% FBS (Gibco, 26140) and antibiotics (Gibco, 15140). SILAC medium was prepared as described previously (Ong & Mann, 2006). In essence, DMEM Glutamax lacking arginine and lysine (a custom preparation from PAA, E15-086) was supplemented with 10 % dialyzed FBS (Sigma, F0392) and antibiotics. Amino acids (84 mg/l $^{13}C_6{}^{15}N_4$ L-arginine plus 146 mg/l $^{13}C_6{}^{15}N_2$ L-lysine or 84 mg/l $^{13}C_6$-L-arginine plus 146 mg/l D_4-L-lysine) were added to obtain „heavy“ and „medium-heavy“ medium, respectively. Labeled amino acids were purchased from Sigma Isotec. The corresponding non-labeled amino acids (Sigma) were used to prepare non-labeled “light” medium.

6.2. Transfection

Plasmids were transfected with Lipofectamine 2000 (Invitrogen), and siRNAs were transfected at a final concentration of 100 nM, using Lipofectamine RNAiMAX (Invitrogen). Controls (mock) contained only the transfection reagent.

6.3. Plasmids

The HNRNPK minigene and the corresponding control plasmid expressing only eGFP were a kind gift from Jun Zhu (NHLBI/NIH, Bethesda, USA). For the PTBP2 minigene, a fragment of the PTBP2 locus containing part of exon 9, whole exon 10 and part of exon 11 was amplified from HeLa genomic DNA using the primers 5’-ACTAAGCTTGTGGGTATGCCTGGAGTC-3’ and 5’-ACTCTCGAGCATCTGTATTAGAGCGCTGTC-3’ and cloned into the control plasmid for HNRNPK. All plasmids were verified by sequencing.

6.4. Western blotting

Total cell lysates in 1x SDS loading buffer (50mM Tris-HCl pH 6.8, 100mM β-mercaptoethanol, 1% SDS, 0.01% bromophenol blue, 10% glycerol) were resolved by 10% SDS-PAGE, proteins were transferred to PVDF membrane using semi-dry blotting apparatus (BioRad) at 2 mA/cm^2. The membrane was blocked in 3% non-fat milk and incubated with primary antibody 1h to overnight, washed with TBST 2 times and incubated with secondary antibody for 30 min to 1h. The protein bands were visualized using ECL reagents (GE Healthcare, RPN2106) and LAS-4000 CCD camera (GE Healthcare). Primary antibodies used were anti-HuR (Santa Cruz, sc-5261 and sc-5483), dilution 1:1000; anti-tubulin (Sigma, T4026), dilution 1:500 in TBST. Secondary antibody was

HRP-conjugated anti-mouse IgG (Abcam, ab6789), dilution 1:1000.

6.5. Transcriptome sequencing

For the technical replicates of the siRNA2 sample, total RNA was extracted twice from the same suspension of cells in Trizol, and all the subsequent steps were performed in parallel. RNA concentration and quality was assessed using NanoDrop ND-1000 UV-VIS Spectrophotometer (Thermo Fisher) and Agilent 2100 Bioanalyzer (RNA 6000 Nano Kit). PolyA+ mRNA was extracted from 1µg total RNA using magnetic Oligo-dT_{25} beads (Invitrogen, 610.05). The eluate was hybridized to the same beads for the second extraction step. The resulting double-purified polyA+ mRNA was used for the sequencing library preparation acccording to the NEBNext mRNA Sample Prep kit (NEB, E6100) instructions, with modifications. The mRNA was eluted from the beads with 17µl of 10mM Tris-HCl (pH 7.5), combined with 4µl of 5x fragmentation buffer, incubated for exactly 3.5 min. at 94ºC and placed on ice. This procedure yields RNA fragments of length 60 to 200 nt. After fragmentation, the RNA was purified using Agencourt RNAClean XP beads (Beckman Genomics) according to manufacturer's procedure. cDNA synthesis, end repair, addition of A overhangs and ligation of the adapters were performed as in NEBNext kit, each followed by purification on AMPure beads (Beckman Genomics). The library was then PCR-amplified using Phusion polymerase (Finnzymes, F-540) for 15 cycles of 10 sec. at 98ºC, 30 sec. at 65ºC and 30 sec. at 72ºC. After purification on AMPure beads, the concentration and quality of the library was assessed by Bioanalyzer (DNA 1000 kit). Libraries were sequenced on Illumina Genome Analyzer GAII or Illumina HiSeq using paired-end protocol.

6.6. Labeling of proteins, sample preparation and measurement by mass spectrometry

Cells were transferred to light SILAC medium 6h post transfection. Two days after transfection siRNA and mock-transfected cells were transferred to medium-heavy and heavy SILAC medium, respectively. After 24h of labeling cells were harvested and equal amounts of siRNA- and mock-transfected cells were combined. Proteins were extracted, separated by SDS-PAGE, trypsin-digested and analyzed by liquid chromatography tandem mass spectrometry (LC-MS/MS) on a high resolution instrument (LTQ-Orbitrap Velos, Thermo Fisher). Raw files were processed by MaxQuant (version 1.0.13.13) for peptide/protein identification at 1% FDR and quantification.

6.7. Small RNA Sequencing

was performed from 10 µg total RNA using the FlashPage Gel system (Ambion) and the standard Illumina small RNA library preparation protocol.

6.8. RIP-PCR

Immunoprecipitations were performed as described for PAR-CLIP. As negative control an anti-FLAG antibody (Sigma, F3165) was used. Typically, 5-10 15cm plates, 50-100µl Protein G beads and 10-20µg antibody were used per IP reaction. RNA was isolated from IP and analyzed by RT-PCR and agarose gel electrophoresis.

6.9. NanoString nCounter Assay

The NanoString nCounter Assay is available as a custom service by NanoString Technologies. Equal amounts (150ng) of RNA isolated from the IP with anti-HuR and anti-FLAG antibodies, as well as total RNA from mock and siRNA-transfected cells were analyzed in parallel using the nCounter Human Cancer Reference Kit (GXA-CR1-12).

6.10. RT-PCR

Trizol isolated RNA was treated with RQ1 DNase (Promega). cDNA synthesis was performed with Superscript III (Invitrogen) with Oligo(dT) (T_{18}NN). PCR amplification was performed using 2x Green DreamTaq Master Mix (Fermentas), 0.5µM of each of the forward and reverse primers, and 1µl of cDNA for 30 cycles of 15 s at 94 ºC, 15 s at 60 ºC, and 20 s at 72ºC.

6.11. Quantification of alternative exon inclusion

After RT-PCR, the products were resolved by 8% TBE-PAGE. In parallel, PCR products were purified by phenol-chloroform extraction and analyzed by Agilent BioAnalyzer DNA 1000 Assay. PSI (Percent Spliced In) values were calculated as the molar ratio of the peak corresponding to the exon containing isoform and the sum of the peaks representing both isoforms.

6.12. PAR-CLIP

The PAR-CLIP method has recently been described (Hafner et al., 2010).

6.12.1. Thionucleoside labeling

HeLa cells were grown in DMEM or in SILAC medium. For a typical experiment, 60-100 15cm plates were used. Stock solution of 4-thiouridine (4SU) (Sigma, T4509) was diluted in water to 1M and kept at -20ºC. Stock solution of 6-thioguanosine (6SG) (Sigma, 858412) was diluted in DMSO to 0.5M and kept at -20ºC. For labeling, 4SU or 6SG was diluted in appropriate medium (DMEM or SILAC) and added to the cells to the final concentration of 100µM. 4SU labeling was accomplished overnight to label long-lived transcripts. After overnight incubation, fresh 4SU solution was added and cells were incubated for additional 4 hours to label short-lived transcripts. For 6SG the overnight step was omitted.

6.12.2. Crosslinking, cell lysis and immunoprecipitation

After labeling, the medium was aspirated from the plates and the cells were crosslinked on ice using Stratalinker (Stratagene) with customized 365nm UV-lamps. (Energy setting 1500 µJ x 100/cm^2). Cells were scraped in cold PBS and pelleted by centrifugation. For lysis, 3 volumes of NP-40 lysis buffer (50 mM HEPES-K pH 7.5, 150 mM KCl, 2 mM EDTA, 0.5% (v/v) NP-40, 0.5 mM DTT, protease inhibitor cocktail (Roche, 11836170001)) was added to the cells followed by 10 min incubation on ice and 10 passes through a syringe with 20G needle. Lysates were cleared by centrifugation (13,000 rpm, 10 min at 4ºC). Cleared lysate was partially digested with RNaseT1 (Fermentas) (final concentration 1U/µl) for 15 min. in a room-temperature water bath, cooled on ice for 5 min and filtered through a 5 µm supor membrane syringe filter (Pall). HuR was immunoprecipitated from filtered cell lysates using antibodies conjugated to magnetic Protein G Dynabeads (Invitrogen). For 1 ml of cell lysate, 25 µl beads and 10 µg of antibody (anti-HuR, Santa Cruz, sc-5261) were used. Lysates were incubated with beads for 1 hour at 4ºC. Beads were washed three times with IP wash buffer (50 mM HEPES-K pH 7.5, 300 mM KCl, 0.5% NP-40, 0.5 mM DTT, protease inhibitor cocktail) and treated with RNase T1 in one volume of IP wash buffer at final concentration of 50 U/µl for exactly 8 min. The beads were immediately washed three times with ice-cold high salt buffer (50 mM HEPES-K pH 7.5, 500 mM KCl, 0.5% NP-40, 0.5 mM DTT, protease inhibitor cocktail). The beads were washed two times with 1x NEB buffer #3 and resuspended in NEB buffer #3 containing 0.5 U/µl Calf Intestinal Phosphatase (NEB). Dephosphorylation was performed at 37ºC in a thermomixer (Eppendorf) with shaking at 1250 rpm for 30 min. Beads were then washed twice with crosslink wash buffer (50 mM Tris-HCl pH 7.5, 20 mM EGTA, 0.5% NP-40) and twice with PNK buffer without DTT (50 mM Tris-HCl pH 7.5, 50 mM NaCl, 10 mM $MgCl_2$) and then labeled with ^{32}P(gamma)-ATP (Perkin-Elmer, NEG 502A) in PNK buffer with 5 mM DTT and T4 polynucleotide kinase (NEB). Gamma-ATP was used at the final concentration of 0.5µCi/µl for 4SU-labeled and 1-2µCi/µl for 6SG-labeled immunoprecipitates. The labeling reaction was carried out at 37ºC with 1250 rpm shaking for 20 min. ATP (Fermentas) was added to a final concentration of 100 µM and the reaction was further incubated for 5 min. The beads were washed 5 times with 800µl PNK buffer without DTT and resuspended in 95 µl of 2x SDS-PAGE loading buffer (20% glycerol (v/v), 160 mM Tris-HCl pH 6.8, 4% SDS (w/v), 200 mM DTT, 0.2% bromophenol blue).

6.12.3. SDS-PAGE and electroelution of RNA

Beads in SDS loading buffer were boiled at 95ºC for 5 min and the supernatant was loaded onto an SDS gel (NuPAGE Novex 4-20% BT Gel, Invitrogen). Gels were exposed for 15 min - 1 hour to a phosphorimaging screen and visualized on FLA 7000 imager (GE healthcare). The radioactive band

corresponding to HuR (37 KDa) was cut out of the gel. HuR-RNA complexes were electroeluted from the gel using D-Tube Dyalyzer Kit MWCO 3.5kDa (Novagen) for 2h at 100V in SDS running buffer (25mM Tris base, 192 mM glycine, 0.1% SDS). The electroeluate (~750 µl) was combined with 2x proteinase K buffer (200 mM Tris-HCl pH 7.5, 150 mM NaCl, 12.5 mM EDTA, 2% SDS) containing proteinase K (Roche, 03115879001) to yield the final concentration of 2 mg/ml. The reaction was incubated at 55ºC for 30 min. Immunoprecipitated RNA was recovered by phenol-chloroform extraction and ethanol precipitation, using GlycoBlue (Ambion).

6.12.4. RNA cloning and sequencing

Sequencing libraries were constructed using the small RNA cloning protocol (Hafner et al., 2008). The PAR-CLIP libraries were sequenced on an Illumina Genome Analyzer GAII using the 36 bp single read protocol.

6.13. Quantitative real-time PCR

For miRNA qPCR, TaqMan miRNA Assays from Applied Biosystems (hsa-miR-7; hsa-let-7b; hsa-rnu6B) and 2x TaqMan Master Mix (Applied Biosystems) were used, according to manufacturer's instructions.

6.14. Northern blotting

100 µg HeLa total RNA was resolved on a midi-size (14x16cm) 15% denaturing polyacrylamide gel (SequaGel Sequencing System Kit, National Diagnostics, EC-833). Radioactively labeled RNA decade markers (Ambion, AM7778) were included. RNA was transferred to Hybond-N+ membrane (GE healthcare) using semi-dry transfer apparatus (Bio-Rad) with 0.5X TBE for 1h at 3 mA/cm^2. The membrane was UV crosslinked twice using auto crosslink setting (1200 J) in Stratalinker UV Crosslinker (Stratagene). The membrane was pre-hybridized for 30 min at 50°C in hybridization solution (5X SSC, 20mM Na_2HPO_4 [pH 7], 1%SDS, 1X Denhardt's solution [Invitrogen], 0.1mg/ml sonicated salmon sperm DNA [Applichem]). (Salmon sperm DNA was denatured for 5 min at 95°C before adding to the solution). 30 pmol of radioactively labeled probe was added to the hybridization solution and hybridization performed overnight at the temperature 10°C below T_m of the probe. The membrane was washed twice for 10 min with wash solution I (5X SSC, 1%SDS) and once with wash solution II (1X SSC, 1%SDS). The membrane was exposed for 1h to overnight to a phosphorimaging screen and visualized on FLA 7000 imager (GE healthcare). Before reprobing the membrane with the U6 loading control, the membrane was stripped 3 times for 10 min in 1% SDS at 80°C.

6.15. Oligonucleotides

6.15.1. Primers

>PTBP2_FL_1
AGCTGGTGGCAATACAGTCC
>PTBP2_FL_2
ATCTTCACACGCTGCACATC
>ZNF207_FL_1
CTAAGCCTCTTTTCCCCAGTG
>ZNF207_FL_2
TACCAACAGGTCCTTGGACAG
>GANAB_FL_1
AGCTGGGTCTTTTGATCCTTG
>GANAB_FL_2
GAGGACCGAAGTCTTTTGCTT
>DST_FL_1
AGTCGCAGTTGCTGGGAGTC
>DST_FL_2
AAAGCGATTTCAAGTTGAGCA
>TNRC6B_F
ATGGGTCAACCTTGAGAACG
>TNRC6B_R
TCATCAGTGGCAAACTCAGC
>EIF4E_F
TGTGGCGCTGTTGTTAATGT
>EIF4E_R
ATTGCTTGACGCAGTCTCCT
>DDX6_F
ATGATCGCTTCAACCTGAAAAG
>DDX6_R
ATGTGTCACAGATCCAAACGAG
>GAPDH_R
GGCATGGACTGTGGTCATGAG
>GAPDH_F
TGCACCACCAACTGCTTAGC
>ELAV1_R
CTGGGGGTTTATGACCATTG

>ELAV1_F
AGGTGATCAAAGACGCCAAC
>MALAT1_F
TGGGGGAGTTTCGTACTGAG
>MALAT1_R
TCTCCAGGACTTGGCAGTCT
>PRKAA1_F
TTGCGTGTACGAAGGAAGAAT
>PRKAA1_R
CCGATCTCTGTGGAGTAGCAG
All the primers were ordered from Biotez (Germany).

6.15.2. siRNAs

Two siRNAs against CDS and 3'UTR of HuR, siRNA1 (sense, 5'-AAGAGGCAAUUACCAGUUUCA-3') and siRNA2 (sense, 5'-AAUCUUAAGUUUCGUAAGUUA-3') (Fernau et al., 2010), were synthesized as custom RNA oligonucleotide duplexes by Sigma Aldrich.

6.15.3. Northern blotting probes

>hsa_U6

TATGGAACGCTTCACGAATTTGCGTGTCAT

Mature miR-7 LNA probe was purchased from Exiqon (411891-00).

6.16. Computational methods

For the description of computational methods, please refer to [107] .

6.17. Zebrafish methods summary.

Zebrafish were maintained at 26.5°C and bred in standard conditions.
The *Tg (fli:egfp)*^{y1} transgenic reporter line was described elsewhere [132].
Morpholino antisense oligonumers were purchased from GeneTools. Morpholinos were prepared according to the manufacturer's protocol and microinjected into the yolk of one cell stage embryos at the concentration of 300μM. For the imaging, embryos were immobilized with 0.16 mg/ml tricaine. Images were taken with the fluorescent microscope Leica MZ16 FA.

The ELAVL1 translation-blocking morpholino sequence was TGTGGTCTTCGTAACCGTTCGACAT.

7. List of publications

Lebedeva S., Jens M., Theil K., Schwanhäusser B., Selbach M., Landthaler M., Rajewsky N. *Transcriptome wide analysis of regulatory interactions of the RNA-binding protein HuR.* Mol.Cell, 2011:43(3):340-52

Friedländer M.R., Adamidi C., Han T., Lebedeva S., Isenbarger T.A., Hirst M., Marra M., Nusbaum C., Lee W.L., Jenkin J.C., Sánchez Alvarado A., Kim J.K., Rajewsky N. *High-resolution profiling and discovery of planarian small RNAs.* Proc Natl Acad Sci U S A. 2009 Jul 14;106(28):11546-51

Song J., Stoeckius M., Maaskola J., Friedlaender M., Juliano C., Lebedeva S., Thompson W., Rajewsky N., Wessel G. *Select microRNAs are essential for early development in the sea urchin.* Dev. Biol. (2011), doi:10.1016/j.ydbio.2011.11.015

8. References

[1]Taniguchi, Y.; Choi, P. J.; Li, G.-W.; Chen, H.; Babu, M.; Hearn, J.; Emili, A. & Xie, X. S. (2010). Quantifying E. coli proteome and transcriptome with single-molecule sensitivity in single cells. Science *329*, 533-538.
[2]de Sousa Abreu, R.; Penalva, L. O.; Marcotte, E. M. & Vogel, C. (2009). Global signatures of protein and mRNA expression levels. Mol Biosyst *5*, 1512-1526.
[3]Schwanhäusser, B.; Busse, D.; Li, N.; Dittmar, G.; Schuchhardt, J.; Wolf, J.; Chen, W. & Selbach, M. (2011). Global quantification of mammalian gene expression control. Nature *473*, 337-342.
[4]Garneau, N. L.; Wilusz, J. & Wilusz, C. J. (2007). The highways and byways of mRNA decay. Nat Rev Mol Cell Biol *8*, 113-126.
[5]Hir, H. L.; Nott, A. & Moore, M. J. (2003). How introns influence and enhance eukaryotic gene expression. Trends Biochem Sci *28*, 215-220.
[6]Besse, F. & Ephrussi, A. (2008). Translational control of localized mRNAs: restricting protein synthesis in space and time. Nat Rev Mol Cell Biol *9*, 971-980.
[7]Farajollahi, S. & Maas, S. (2010). Molecular diversity through RNA editing: a balancing act. Trends Genet *26*, 221-230.
[8]Friedländer, M. R.; Mackowiak, S. D.; Li, N.; Chen, W. & Rajewsky, N. (2011). miRDeep2 accurately identifies known and hundreds of novel microRNA
genes in seven animal clades. Nucleic Acids Res. *(accepted)*.
[9]Lall, S.; Grün, D.; Krek, A.; Chen, K.; Wang, Y.-L.; Dewey, C. N.; Sood, P.; Colombo, T.; Bray, N.; Macmenamin, P.; Kao, H.-L.; Gunsalus, K. C.; Pachter, L.; Piano, F. & Rajewsky, N. (2006). A genome-wide map of conserved microRNA targets in C. elegans. Curr Biol *16*, 460-471.
[10]Krek, A.; Grün, D.; Poy, M. N.; Wolf, R.; Rosenberg, L.; Epstein, E. J.; MacMenamin, P.; da Piedade, I.; Gunsalus, K. C.; Stoffel, M. & Rajewsky, N. (2005). Combinatorial microRNA target predictions. Nat Genet *37*, 495-500.
[11]Friedman, R. C.; Farh, K. K.-H.; Burge, C. B. & Bartel, D. P. (2009). Most mammalian mRNAs are conserved targets of microRNAs. Genome Res *19*, 92-105.
[12]Darnell, R. B. (2010). HITS-CLIP: panoramic views of protein–RNA regulation in living cells. Wiley Interdisciplinary Reviews: RNA *1*, 266–286.
[13]Hafner, M.; Landthaler, M.; Burger, L.; Khorshid, M.; Hausser, J.; Berninger, P.; Rothballer, A.; Ascano, M.; Jungkamp, A.-C.; Munschauer, M.; Ulrich, A.; Wardle, G. S.; Dewell, S.; Zavolan, M. & Tuschl, T. (2010). Transcriptome-wide identification of RNA-binding protein and microRNA target sites by PAR-CLIP. Cell *141*, 129-141.
[14]König, J.; Zarnack, K.; Rot, G.; Curk, T.; Kayikci, M.; Zupan, B.; Turner, D. J.; Luscombe, N. M. & Ule, J. (2010). iCLIP reveals the function of hnRNP particles in splicing at individual nucleotide resolution. Nat Struct Mol Biol *17*, 909-915.
[15]Mayr, C. & Bartel, D. P. (2009). Widespread shortening of 3'UTRs by alternative cleavage and polyadenylation activates oncogenes in cancer cells. Cell *138*, 673-684.
[16]Keene, J. D. (2007). RNA regulons: coordination of post-transcriptional events. Nat Rev Genet *8*, 533-543.
[17]Hornstein, E. & Shomron, N. (2006). Canalization of development by microRNAs. Nat Genet *38 Suppl*, S20-S24.
[18]Giraldez, A. J.; Mishima, Y.; Rihel, J.; Grocock, R. J.; Dongen, S. V.; Inoue, K.; Enright, A. J. & Schier, A. F. (2006). Zebrafish MiR-430 promotes deadenylation and clearance of maternal mRNAs. Science *312*, 75-79.
[19]Penalva, L. O. F. & Sánchez, L. (2003). RNA binding protein sex-lethal (Sxl) and control of Drosophila sex determination and dosage compensation. Microbiol Mol Biol Rev *67*, 343-59, table of contents.
[20]Lunde, B. M.; Moore, C. & Varani, G. (2007). RNA-binding proteins: modular design for

efficient function. Nat Rev Mol Cell Biol *8*, 479-490.
[21]Nagy, E. & Rigby, W. F. (1995). Glyceraldehyde-3-phosphate dehydrogenase selectively binds AU-rich RNA in the NAD(+)-binding region (Rossmann fold). J Biol Chem *270*, 2755-2763.
[22]Scherrer, T.; Mittal, N.; Janga, S. C. & Gerber, A. P. (2010). A screen for RNA-binding proteins in yeast indicates dual functions for many enzymes. PLoS One *5*, e15499.
[23]Wightman, B.; Ha, I. & Ruvkun, G. (1993). Posttranscriptional regulation of the heterochronic gene lin-14 by lin-4 mediates temporal pattern formation in C. elegans. Cell *75*, 855-862.
[24]Tolia, N. H. & Joshua-Tor, L. (2007). Slicer and the argonautes. Nat Chem Biol *3*, 36-43.
[25]Bartel, D. P. (2009). MicroRNAs: target recognition and regulatory functions. Cell *136*, 215-233.
[26]Winter, J.; Jung, S.; Keller, S.; Gregory, R. I. & Diederichs, S. (2009). Many roads to maturity: microRNA biogenesis pathways and their regulation. Nat Cell Biol *11*, 228-234.
[27]Friedländer, M. R.; Chen, W.; Adamidi, C.; Maaskola, J.; Einspanier, R.; Knespel, S. & Rajewsky, N. (2008). Discovering microRNAs from deep sequencing data using miRDeep. Nat Biotechnol *26*, 407-415.
[28]Gallie, D. R. (1998). A tale of two termini: a functional interaction between the termini of an mRNA is a prerequisite for efficient translation initiation. Gene *216*, 1-11.
[29]Filipowicz, W.; Bhattacharyya, S. N. & Sonenberg, N. (2008). Mechanisms of post-transcriptional regulation by microRNAs: are the answers in sight? Nat Rev Genet *9*, 102-114.
[30]Huntzinger, E. & Izaurralde, E. (2011). Gene silencing by microRNAs: contributions of translational repression and mRNA decay. Nat Rev Genet *12*, 99-110.
[31]Selbach, M.; Schwanhäusser, B.; Thierfelder, N.; Fang, Z.; Khanin, R. & Rajewsky, N. (2008). Widespread changes in protein synthesis induced by microRNAs. Nature *455*, 58-63.
[32]Guo, H.; Ingolia, N. T.; Weissman, J. S. & Bartel, D. P. (2010). Mammalian microRNAs predominantly act to decrease target mRNA levels. Nature *466*, 835-840.
[33]Mukherji, S.; Ebert, M. S.; Zheng, G. X. Y.; Tsang, J. S.; Sharp, P. A. & van Oudenaarden, A. (2011). MicroRNAs can generate thresholds in target gene expression. Nat Genet *43*, 854-859.
[34]Eulalio, A.; Tritschler, F. & Izaurralde, E. (2009). The GW182 protein family in animal cells: new insights into domains required for miRNA-mediated gene silencing. RNA *15*, 1433-1442.
[35]Braun, J. E.; Huntzinger, E.; Fauser, M. & Izaurralde, E. (2011). GW182 Proteins Directly Recruit Cytoplasmic Deadenylase Complexes to miRNA Targets. Mol Cell *44*, 120-133.
[36]Bhattacharyya, S. N.; Habermacher, R.; Martine, U.; Closs, E. I. & Filipowicz, W. (2006). Relief of microRNA-mediated translational repression in human cells subjected to stress. Cell *125*, 1111-1124.
[37]Fan, X. C.; Myer, V. E. & Steitz, J. A. (1997). AU-rich elements target small nuclear RNAs as well as mRNAs for rapid degradation. Genes Dev *11*, 2557-2568.
[38]Chen, C. Y.; Gherzi, R.; Ong, S. E.; Chan, E. L.; Raijmakers, R.; Pruijn, G. J.; Stoecklin, G.; Moroni, C.; Mann, M. & Karin, M. (2001). AU binding proteins recruit the exosome to degrade ARE-containing mRNAs. Cell *107*, 451-464.
[39]Kedde, M.; van Kouwenhove, M.; Zwart, W.; Vrielink, J. A. F. O.; Elkon, R. & Agami, R. (2010). A Pumilio-induced RNA structure switch in p27-3' UTR controls miR-221 and miR-222 accessibility. Nat Cell Biol *12*, 1014-1020.
[40]Franks, T. M. & Lykke-Andersen, J. (2007). TTP and BRF proteins nucleate processing body formation to silence mRNAs with AU-rich elements. Genes Dev *21*, 719-735.
[41]Suswam, E. A.; Nabors, L. B.; Huang, Y.; Yang, X. & King, P. H. (2005). IL-1beta induces stabilization of IL-8 mRNA in malignant breast cancer cells via the 3' untranslated region: Involvement of divergent RNA-binding factors HuR, KSRP and TIAR. Int J Cancer *113*, 911-919.
[42]Vardy, L. & Orr-Weaver, T. L. (2007). Regulating translation of maternal messages: multiple repression mechanisms. Trends Cell Biol *17*, 547-554.
[43]Richter, J. D. (2007). CPEB: a life in translation. Trends Biochem Sci *32*, 279-285.

[44]Arthur, P. K.; Claussen, M.; Koch, S.; Tarbashevich, K.; Jahn, O. & Pieler, T. (2009). Participation of Xenopus Elr-type proteins in vegetal mRNA localization during oogenesis. J Biol Chem *284*, 19982-19992.
[45]Kim, H. H.; Abdelmohsen, K.; Lal, A.; Pullmann, R.; Yang, X.; Galban, S.; Srikantan, S.; Martindale, J. L.; Blethrow, J.; Shokat, K. M. & Gorospe, M. (2008). Nuclear HuR accumulation through phosphorylation by Cdk1. Genes Dev *22*, 1804-1815.
[46]Johnson, B. A.; Stehn, J. R.; Yaffe, M. B. & Blackwell, T. K. (2002). Cytoplasmic localization of tristetraprolin involves 14-3-3-dependent and -independent mechanisms. J Biol Chem *277*, 18029-18036.
[47]Shen, Z.-J.; Esnault, S. & Malter, J. S. (2005). The peptidyl-prolyl isomerase Pin1 regulates the stability of granulocyte-macrophage colony-stimulating factor mRNA in activated eosinophils. Nat Immunol *6*, 1280-1287.
[48]Briata, P.; Forcales, S. V.; Ponassi, M.; Corte, G.; Chen, C.-Y.; Karin, M.; Puri, P. L. & Gherzi, R. (2005). p38-dependent phosphorylation of the mRNA decay-promoting factor KSRP controls the stability of select myogenic transcripts. Mol Cell *20*, 891-903.
[49]Figueroa, A.; Cuadrado, A.; Fan, J.; Atasoy, U.; Muscat, G. E.; Muñoz-Canoves, P.; Gorospe, M. & Muñoz, A. (2003). Role of HuR in skeletal myogenesis through coordinate regulation of muscle differentiation genes. Mol Cell Biol *23*, 4991-5004.
[50]Lal, A.; Mazan-Mamczarz, K.; Kawai, T.; Yang, X.; Martindale, J. L. & Gorospe, M. (2004). Concurrent versus individual binding of HuR and AUF1 to common labile target mRNAs. EMBO J *23*, 3092-3102.
[51]Kawai, T.; Lal, A.; Yang, X.; Galban, S.; Mazan-Mamczarz, K. & Gorospe, M. (2006). Translational control of cytochrome c by RNA-binding proteins TIA-1 and HuR. Mol Cell Biol *26*, 3295-3307.
[52]Salmena, L.; Poliseno, L.; Tay, Y.; Kats, L. & Pandolfi, P. P. (2011). A ceRNA Hypothesis: The Rosetta Stone of a Hidden RNA Language? Cell *146*, 353-358.
[53]Kedde, M.; Strasser, M. J.; Boldajipour, B.; Vrielink, J. A. F. O.; Slanchev, K.; le Sage, C.; Nagel, R.; Voorhoeve, P. M.; van Duijse, J.; Ørom, U. A.; Lund, A. H.; Perrakis, A.; Raz, E. & Agami, R. (2007). RNA-binding protein Dnd1 inhibits microRNA access to target mRNA. Cell *131*, 1273-1286.
[54]Huang, J.; Liang, Z.; Yang, B.; Tian, H.; Ma, J. & Zhang, H. (2007). Derepression of microRNA-mediated protein translation inhibition by apolipoprotein B mRNA-editing enzyme catalytic polypeptide-like 3G (APOBEC3G) and its family members. J Biol Chem *282*, 33632-33640.
[55]Srikantan, S.; Abdelmohsen, K.; Lee, E. K.; Tominaga, K.; Subaran, S. S.; Kuwano, Y.; Kulshrestha, R.; Panchakshari, R.; Kim, H. H.; Yang, X.; Martindale, J. L.; Marasa, B. S.; Kim, M. M.; Wersto, R. P.; Indig, F. E.; Chowdhury, D. & Gorospe, M. (2011). Translational control of Top2A influences doxorubicin efficacy. Mol Cell Biol .
[56]Kim, H. H.; Kuwano, Y.; Srikantan, S.; Lee, E. K.; Martindale, J. L. & Gorospe, M. (2009). HuR recruits let-7/RISC to repress c-Myc expression. Genes Dev *23*, 1743-1748.
[57]Glorian, V.; Maillot, G.; Polès, S.; Iacovoni, J. S.; Favre, G. & Vagner, S. (2011). HuR-dependent loading of miRNA RISC to the mRNA encoding the Ras-related small GTPase RhoB controls its translation during UV-induced apoptosis. Cell Death Differ .
[58]Viswanathan, S. R.; Daley, G. Q. & Gregory, R. I. (2008). Selective blockade of microRNA processing by Lin28. Science *320*, 97-100.
[59]Rybak, A.; Fuchs, H.; Smirnova, L.; Brandt, C.; Pohl, E. E.; Nitsch, R. & Wulczyn, F. G. (2008). A feedback loop comprising lin-28 and let-7 controls pre-let-7 maturation during neural stem-cell commitment. Nat Cell Biol *10*, 987-993.
[60]Guil, S. & Cáceres, J. F. (2007). The multifunctional RNA-binding protein hnRNP A1 is required for processing of miR-18a. Nat Struct Mol Biol *14*, 591-596.

[61]Wu, H.; Sun, S.; Tu, K.; Gao, Y.; Xie, B.; Krainer, A. R. & Zhu, J. (2010). A splicing-independent function of SF2/ASF in microRNA processing. Mol Cell *38*, 67-77.
[62]Eiring, A. M.; Harb, J. G.; Neviani, P.; Garton, C.; Oaks, J. J.; Spizzo, R.; Liu, S.; Schwind, S.; Santhanam, R.; Hickey, C. J.; Becker, H.; Chandler, J. C.; Andino, R.; Cortes, J.; Hokland, P.; Huettner, C. S.; Bhatia, R.; Roy, D. C.; Liebhaber, S. A.; Caligiuri, M. A.; Marcucci, G.; Garzon, R.; Croce, C. M.; Calin, G. A. & Perrotti, D. (2010). miR-328 functions as an RNA decoy to modulate hnRNP E2 regulation of mRNA translation in leukemic blasts. Cell *140*, 652-665.
[63]Wang, E. T.; Sandberg, R.; Luo, S.; Khrebtukova, I.; Zhang, L.; Mayr, C.; Kingsmore, S. F.; Schroth, G. P. & Burge, C. B. (2008). Alternative isoform regulation in human tissue transcriptomes. Nature *456*, 470-476.
[64]Zhu, H.; Hinman, M. N.; Hasman, R. A.; Mehta, P. & Lou, H. (2008). Regulation of neuron-specific alternative splicing of neurofibromatosis type 1 pre-mRNA. Mol Cell Biol *28*, 1240-1251.
[65]Zhu, H.; Hasman, R. A.; Barron, V. A.; Luo, G. & Lou, H. (2006). A nuclear function of Hu proteins as neuron-specific alternative RNA processing regulators. Mol Biol Cell *17*, 5105-5114.
[66]Weinmann, L.; Höck, J.; Ivacevic, T.; Ohrt, T.; Mütze, J.; Schwille, P.; Kremmer, E.; Benes, V.; Urlaub, H. & Meister, G. (2009). Importin 8 is a gene silencing factor that targets argonaute proteins to distinct mRNAs. Cell *136*, 496-507.
[67]Liao, J.-Y.; Ma, L.-M.; Guo, Y.-H.; Zhang, Y.-C.; Zhou, H.; Shao, P.; Chen, Y.-Q. & Qu, L.-H. (2010). Deep sequencing of human nuclear and cytoplasmic small RNAs reveals an unexpectedly complex subcellular distribution of miRNAs and tRNA 3' trailers. PLoS One *5*, e10563.
[68]Alló, M.; Buggiano, V.; Fededa, J. P.; Petrillo, E.; Schor, I.; de la Mata, M.; Agirre, E.; Plass, M.; Eyras, E.; Elela, S. A.; Klinck, R.; Chabot, B. & Kornblihtt, A. R. (2009). Control of alternative splicing through siRNA-mediated transcriptional gene silencing. Nat Struct Mol Biol *16*, 717-724.
[69]Sekii, K.; Salvenmoser, W.; Mulder, K. D.; Scharer, L. & Ladurner, P. (2009). Melav2, an elav-like gene, is essential for spermatid differentiation in the flatworm Macrostomum lignano. BMC Dev Biol *9*, 62.
[70]Fan, X. C. & Steitz, J. A. (1998). HNS, a nuclear-cytoplasmic shuttling sequence in HuR. Proc Natl Acad Sci U S A *95*, 15293-15298.
[71]Kasashima, K.; Terashima, K.; Yamamoto, K.; Sakashita, E. & Sakamoto, H. (1999). Cytoplasmic localization is required for the mammalian ELAV-like protein HuD to induce neuronal differentiation. Genes Cells *4*, 667-683.
[72]Park, S.; Myszka, D. G.; Yu, M.; Littler, S. J. & Laird-Offringa, I. A. (2000). HuD RNA recognition motifs play distinct roles in the formation of a stable complex with AU-rich RNA. Mol Cell Biol *20*, 4765-4772.
[73]Toba, G. & White, K. (2008). The third RNA recognition motif of Drosophila ELAV protein has a role in multimerization. Nucleic Acids Res *36*, 1390-1399.
[74]Meisner, N.-C.; Hintersteiner, M.; Seifert, J.-M.; Bauer, R.; Benoit, R. M.; Widmer, A.; Schindler, T.; Uhl, V.; Lang, M.; Gstach, H. & Auer, M. (2009). Terminal adenosyl transferase activity of posttranscriptional regulator HuR revealed by confocal on-bead screening. J Mol Biol *386*, 435-450.
[75]Lu, J.-Y. & Schneider, R. J. (2004). Tissue distribution of AU-rich mRNA-binding proteins involved in regulation of mRNA decay. J Biol Chem *279*, 12974-12979.
[76]Campos, A. R.; Grossman, D. & White, K. (1985). Mutant alleles at the locus elav in Drosophila melanogaster lead to nervous system defects. A developmental-genetic analysis. J Neurogenet *2*, 197-218.
[77]Katsanou, V.; Milatos, S.; Yiakouvaki, A.; Sgantzis, N.; Kotsoni, A.; Alexiou, M.; Harokopos, V.; Aidinis, V.; Hemberger, M. & Kontoyiannis, D. L. (2009). The RNA-binding protein Elavl1/HuR is essential for placental branching morphogenesis and embryonic development. Mol Cell Biol *29*, 2762-2776.
[78]Chi, M. N.; Auriol, J.; Jégou, B.; Kontoyiannis, D. L.; Turner, J. M. A.; de Rooij, D. G. &

Morello, D. (2011). The RNA-binding protein ELAVL1/HuR is essential for mouse spermatogenesis, acting both at meiotic and postmeiotic stages. Mol Biol Cell *22*, 2875-2885.
[79]Papadaki, O.; Milatos, S.; Grammenoudi, S.; Mukherjee, N.; Keene, J. D. & Kontoyiannis, D. L. (2009). Control of thymic T cell maturation, deletion and egress by the RNA-binding protein HuR. J Immunol *182*, 6779-6788.
[80]Gantt, K. R.; Cherry, J.; Richardson, M.; Karschner, V.; Atasoy, U. & Pekala, P. H. (2006). The regulation of glucose transporter (GLUT1) expression by the RNA binding protein HuR. J Cell Biochem *99*, 565-574.
[81]Wang, W.; Caldwell, M. C.; Lin, S.; Furneaux, H. & Gorospe, M. (2000). HuR regulates cyclin A and cyclin B1 mRNA stability during cell proliferation. EMBO J *19*, 2340-2350.
[82]Dormoy-Raclet, V.; Ménard, I.; Clair, E.; Kurban, G.; Mazroui, R.; Marco, S. D.; von Roretz, C.; Pause, A. & Gallouzi, I.-E. (2007). The RNA-binding protein HuR promotes cell migration and cell invasion by stabilizing the beta-actin mRNA in a U-rich-element-dependent manner. Mol Cell Biol *27*, 5365-5380.
[83]Abdelmohsen, K.; Srikantan, S.; Kuwano, Y. & Gorospe, M. (2008). miR-519 reduces cell proliferation by lowering RNA-binding protein HuR levels. Proc Natl Acad Sci U S A *105*, 20297-20302.
[84]Katsanou, V.; Papadaki, O.; Milatos, S.; Blackshear, P. J.; Anderson, P.; Kollias, G. & Kontoyiannis, D. L. (2005). HuR as a negative posttranscriptional modulator in inflammation. Mol Cell *19*, 777-789.
[85]Gallouzi, I. E.; Brennan, C. M.; Stenberg, M. G.; Swanson, M. S.; Eversole, A.; Maizels, N. & Steitz, J. A. (2000). HuR binding to cytoplasmic mRNA is perturbed by heat shock. Proc Natl Acad Sci U S A *97*, 3073-3078.
[86]Wang, W.; Furneaux, H.; Cheng, H.; Caldwell, M. C.; Hutter, D.; Liu, Y.; Holbrook, N. & Gorospe, M. (2000). HuR regulates p21 mRNA stabilization by UV light. Mol Cell Biol *20*, 760-769.
[87]Westmark, C. J.; Bartleson, V. B. & Malter, J. S. (2005). RhoB mRNA is stabilized by HuR after UV light. Oncogene *24*, 502-511.
[88]Izquierdo, J. M. (2010). Cell-specific regulation of Fas exon 6 splicing mediated by Hu antigen R. Biochem Biophys Res Commun .
[89]Amadio, M.; Scapagnini, G.; Laforenza, U.; Intrieri, M.; Romeo, L.; Govoni, S. & Pascale, A. (2008). Post-transcriptional regulation of HSP70 expression following oxidative stress in SH-SY5Y cells: the potential involvement of the RNA-binding protein HuR. Curr Pharm Des *14*, 2651-2658.
[90]Tran, H.; Maurer, F. & Nagamine, Y. (2003). Stabilization of urokinase and urokinase receptor mRNAs by HuR is linked to its cytoplasmic accumulation induced by activated mitogen-activated protein kinase-activated protein kinase 2. Mol Cell Biol *23*, 7177-7188.
[91]Abdelmohsen, K.; Pullmann, R.; Lal, A.; Kim, H. H.; Galban, S.; Yang, X.; Blethrow, J. D.; Walker, M.; Shubert, J.; Gillespie, D. A.; Furneaux, H. & Gorospe, M. (2007). Phosphorylation of HuR by Chk2 regulates SIRT1 expression. Mol Cell *25*, 543-557.
[92]Brennan, C. M. & Steitz, J. A. (2001). HuR and mRNA stability. Cell Mol Life Sci *58*, 266-277.
[93]Meng, Z.; King, P. H.; Nabors, L. B.; Jackson, N. L.; Chen, C.-Y.; Emanuel, P. D. & Blume, S. W. (2005). The ELAV RNA-stability factor HuR binds the 5'-untranslated region of the human IGF-IR transcript and differentially represses cap-dependent and IRES-mediated translation. Nucleic Acids Res *33*, 2962-2979.
[94]Galbán, S.; Kuwano, Y.; Pullmann, R.; Martindale, J. L.; Kim, H. H.; Lal, A.; Abdelmohsen, K.; Yang, X.; Dang, Y.; Liu, J. O.; Lewis, S. M.; Holcik, M. & Gorospe, M. (2008). RNA-binding proteins HuR and PTB promote the translation of hypoxia-inducible factor 1alpha. Mol Cell Biol *28*, 93-107.
[95]Kullmann, M.; Göpfert, U.; Siewe, B. & Hengst, L. (2002). ELAV/Hu proteins inhibit p27

translation via an IRES element in the p27 5'UTR. Genes Dev *16*, 3087-3099.
[96]Kim, H. H. & Gorospe, M. (2008). Phosphorylated HuR shuttles in cycles. Cell Cycle *7*, 3124-3126.
[97]Yuan, Z.; Sanders, A. J.; Ye, L. & Jiang, W. G. (2010). HuR, a key post-transcriptional regulator, and its implication in progression of breast cancer. Histol Histopathol *25*, 1331-1340.
[98]Kedersha, N. & Anderson, P. (2002). Stress granules: sites of mRNA triage that regulate mRNA stability and translatability. Biochem Soc Trans *30*, 963-969.
[99]Chi, M. N.; Chalmel, F.; Agius, E.; Vanzo, N.; Khabar, K. S. A.; Jégou, B. & Morello, D. (2009). Temporally regulated traffic of HuR and its associated ARE-containing mRNAs from the chromatoid body to polysomes during mouse spermatogenesis. PLoS One *4*, e4900.
[100]Mili, S. & Steitz, J. A. (2004). Evidence for reassociation of RNA-binding proteins after cell lysis: implications for the interpretation of immunoprecipitation analyses. RNA *10*, 1692-1694.
[101]Keene, J. D.; Komisarow, J. M. & Friedersdorf, M. B. (2006). RIP-Chip: the isolation and identification of mRNAs, microRNAs and protein components of ribonucleoprotein complexes from cell extracts. Nat Protoc *1*, 302-307.
[102]Niranjanakumari, S.; Lasda, E.; Brazas, R. & Garcia-Blanco, M. A. (2002). Reversible cross-linking combined with immunoprecipitation to study RNA-protein interactions in vivo. Methods *26*, 182-190.
[103]Ule, J.; Jensen, K. B.; Ruggiu, M.; Mele, A.; Ule, A. & Darnell, R. B. (2003). CLIP identifies Nova-regulated RNA networks in the brain. Science *302*, 1212-1215.
[104]Testa, S. M.; Disney, M. D.; Turner, D. H. & Kierzek, R. (1999). Thermodynamics of RNA-RNA duplexes with 2- or 4-thiouridines: implications for antisense design and targeting a group I intron. Biochemistry *38*, 16655-16662.
[105]Miller, M. R.; Robinson, K. J.; Cleary, M. D. & Doe, C. Q. (2009). TU-tagging: cell type-specific RNA isolation from intact complex tissues. Nat Methods *6*, 439-441.
[106]Hinman, M. N. & Lou, H. (2008). Diverse molecular functions of Hu proteins. Cell Mol Life Sci *65*, 3168-3181.
[107]Lebedeva, S.; Jens, M.; Theil, K.; Schwanhäusser, B.; Selbach, M.; Landthaler, M. & Rajewsky, N. (2011). Transcriptome-wide Analysis of Regulatory Interactions of the RNA-Binding Protein HuR. Mol Cell .
[108]Geiss, G. K.; Bumgarner, R. E.; Birditt, B.; Dahl, T.; Dowidar, N.; Dunaway, D. L.; Fell, H. P.; Ferree, S.; George, R. D.; Grogan, T.; James, J. J.; Maysuria, M.; Mitton, J. D.; Oliveri, P.; Osborn, J. L.; Peng, T.; Ratcliffe, A. L.; Webster, P. J.; Davidson, E. H.; Hood, L. & Dimitrov, K. (2008). Direct multiplexed measurement of gene expression with color-coded probe pairs. Nat Biotechnol *26*, 317-325.
[109]de Silanes, I. L.; Zhan, M.; Lal, A.; Yang, X. & Gorospe, M. (2004). Identification of a target RNA motif for RNA-binding protein HuR. Proc Natl Acad Sci U S A *101*, 2987-2992.
[110]Meisner, N.-C.; Hackermüller, J.; Uhl, V.; Aszódi, A.; Jaritz, M. & Auer, M. (2004). mRNA openers and closers: modulating AU-rich element-controlled mRNA stability by a molecular switch in mRNA secondary structure. Chembiochem *5*, 1432-1447.
[111]Ray, D.; Kazan, H.; Chan, E. T.; Castillo, L. P.; Chaudhry, S.; Talukder, S.; Blencowe, B. J.; Morris, Q. & Hughes, T. R. (2009). Rapid and systematic analysis of the RNA recognition specificities of RNA-binding proteins. Nat Biotechnol *27*, 667-670.
[112]Benoit, R. M.; Meisner, N.-C.; Kallen, J.; Graff, P.; Hemmig, R.; Cèbe, R.; Ostermeier, C.; Widmer, H. & Auer, M. (2010). The x-ray crystal structure of the first RNA recognition motif and site-directed mutagenesis suggest a possible HuR redox sensing mechanism. J Mol Biol *397*, 1231-1244.
[113]Wang, X. & Hall, T. M. T. (2001). Structural basis for recognition of AU-rich element RNA by the HuD protein. Nat Struct Biol *8*, 141-145.
[114]Larsson, E.; Sander, C. & Marks, D. (2010). mRNA turnover rate limits siRNA and microRNA

efficacy. Mol Syst Biol *6*, 433.
[115]Trapnell, C.; Pachter, L. & Salzberg, S. L. (2009). TopHat: discovering splice junctions with RNA-Seq. Bioinformatics *25*, 1105-1111.
[116]Bussemaker, H. J.; Li, H. & Siggia, E. D. (2001). Regulatory element detection using correlation with expression. Nat Genet *27*, 167-171.
[117]Ong, S.-E. & Mann, M. (2006). A practical recipe for stable isotope labeling by amino acids in cell culture (SILAC). Nat Protoc *1*, 2650-2660.
[118]Trabucchi, M.; Briata, P.; Garcia-Mayoral, M.; Haase, A. D.; Filipowicz, W.; Ramos, A.; Gherzi, R. & Rosenfeld, M. G. (2009). The RNA-binding protein KSRP promotes the biogenesis of a subset of microRNAs. Nature *459*, 1010-1014.
[119]Aboobaker, A. A.; Tomancak, P.; Patel, N.; Rubin, G. M. & Lai, E. C. (2005). Drosophila microRNAs exhibit diverse spatial expression patterns during embryonic development. Proc Natl Acad Sci U S A *102*, 18017-18022.
[120]Wienholds, E.; Kloosterman, W. P.; Miska, E.; Alvarez-Saavedra, E.; Berezikov, E.; de Bruijn, E.; Horvitz, H. R.; Kauppinen, S. & Plasterk, R. H. A. (2005). MicroRNA expression in zebrafish embryonic development. Science *309*, 310-311.
[121]Landgraf, P.; Rusu, M.; Sheridan, R.; Sewer, A.; Iovino, N.; Aravin, A.; Pfeffer, S.; Rice, A.; Kamphorst, A. O.; Landthaler, M.; Lin, C.; Socci, N. D.; Hermida, L.; Fulci, V.; Chiaretti, S.; Foà, R.; Schliwka, J.; Fuchs, U.; Novosel, A.; Müller, R.-U.; Schermer, B.; Bissels, U.; Inman, J.; Phan, Q.; Chien, M.; Weir, D. B.; Choksi, R.; Vita, G. D.; Frezzetti, D.; Trompeter, H.-I.; Hornung, V.; Teng, G.; Hartmann, G.; Palkovits, M.; Lauro, R. D.; Wernet, P.; Macino, G.; Rogler, C. E.; Nagle, J. W.; Ju, J.; Papavasiliou, F. N.; Benzing, T.; Lichter, P.; Tam, W.; Brownstein, M. J.; Bosio, A.; Borkhardt, A.; Russo, J. J.; Sander, C.; Zavolan, M. & Tuschl, T. (2007). A mammalian microRNA expression atlas based on small RNA library sequencing. Cell *129*, 1401-1414.
[122]Papadopoulou, C.; Patrinou-Georgoula, M. & Guialis, A. (2010). Extensive association of HuR with hnRNP proteins within immunoselected hnRNP and mRNP complexes. Biochim Biophys Acta *1804*, 692-703.
[123]Fan, X. C. & Steitz, J. A. (1998). Overexpression of HuR, a nuclear-cytoplasmic shuttling protein, increases the in vivo stability of ARE-containing mRNAs. EMBO J *17*, 3448-3460.
[124]Mukherjee, N.; Corcoran, D. L.; Nusbaum, J. D.; Reid, D. W.; Georgiev, S.; Hafner, M.; Ascano, M.; Tuschl, T.; Ohler, U. & Keene, J. D. (2011). Integrative Regulatory Mapping Indicates that the RNA-Binding Protein HuR Couples Pre-mRNA Processing and mRNA Stability. Mol Cell .
[125]Kishore, S.; Jaskiewicz, L.; Burger, L.; Hausser, J.; Khorshid, M. & Zavolan, M. (2011). A quantitative analysis of CLIP methods for identifying binding sites of RNA-binding proteins. Nat Methods *8*, 559-564.
[126]Dölken, L.; Ruzsics, Z.; Rädle, B.; Friedel, C. C.; Zimmer, R.; Mages, J.; Hoffmann, R.; Dickinson, P.; Forster, T.; Ghazal, P. & Koszinowski, U. H. (2008). High-resolution gene expression profiling for simultaneous kinetic parameter analysis of RNA synthesis and decay. RNA *14*, 1959-1972.
[127]Grimson, A.; Farh, K. K.-H.; Johnston, W. K.; Garrett-Engele, P.; Lim, L. P. & Bartel, D. P. (2007). MicroRNA targeting specificity in mammals: determinants beyond seed pairing. Mol Cell *27*, 91-105.
[128]Spellman, R.; Llorian, M. & Smith, C. W. J. (2007). Crossregulation and functional redundancy between the splicing regulator PTB and its paralogs nPTB and ROD1. Mol Cell *27*, 420-434.
[129]Koushika, S. P.; Lisbin, M. J. & White, K. (1996). ELAV, a Drosophila neuron-specific protein, mediates the generation of an alternatively spliced neural protein isoform. Curr Biol *6*, 1634-1641.
[130]Soller, M. & White, K. (2005). ELAV multimerizes on conserved AU4-6 motifs important for ewg splicing regulation. Mol Cell Biol *25*, 7580-7591.

[131]Baek, D.; Villén, J.; Shin, C.; Camargo, F. D.; Gygi, S. P. & Bartel, D. P. (2008). The impact of microRNAs on protein output. Nature *455*, 64-71.
[132]Lawson, N. D. & Weinstein, B. M. (2002). In vivo imaging of embryonic vascular development using transgenic zebrafish. Dev Biol *248*, 307-318.
[133] Jungkamp, A.C.; Stoeckius, M.; Mecenas, D.; Grün, D.; Mastrobuoni, G.; Kempa, S.; Rajewsky N. (2011). In Vivo and Transcriptome-wide Identification of RNA Binding Protein Target Sites. Mol Cell *44(5)*:828-40.

A1. Appendix. List of literature validated human HuR target genes

ACTB	Dormoy-Raclet et al., 2007
ATF3	Pan et al., 2005
BRCA1	Saunus et al., 2008
FOS	Ma et al., 1996
CCNA2	Wang et al., 2000
CCNB1	Wang et al., 2000
CCND1	Lal et al., 2004
CCNE1	Guo & Hartley 2006
CD247	Moulton et al., 2008
CDKN1A	Lafarga et al., 2009
CDKN1B	Kullmann et al., 2002
CYCS	Kawai et al., 2006
DNMT3B	de Silanes et al., 2009
DUSP1	Kuwano et al., 2008
EIF4E	Topisirovic et al., 2009
ELAVL1	Al-Ahmadi et al., 2009
FAS	Izquierdo 2010
GATA3	Licata et al., 2010
HMOX1	Kuwano et al., 2009
GADD45B	Kuwano et al., 2009
CHIC2	Kuwano et al., 2009
KLF10	Kuwano et al., 2009
ID3	Kuwano et al., 2009
RGS2	Kuwano et al., 2009
HSPA1A	Amadio et al., 2008
IGF1R	Meng et al., 2005
MYC	Kim et al., 2009
NOS2	Rodriguez-Pascual et al., 2000
PLAUR	Tran et al., 2003
PLAU	Tran et al., 2003
PTMA	Lal et al., 2005
PTGS2	Sengupta et al., 2003
RHOB	Westmark et al., 2005
SIRT1	Abdelmohsen et al., 2007
SLC7A1	Bhattacharyya et al., 2006
SNAI1	Dong et al., 2007

TP53	Mazan-Mamczarz et al., 2003
VEGFA	Levy et al., 1998
WNT5A	Leandersson et al.,2006
BCL2	Abdelmohsen et al., 2007
MCL1	Abdelmohsen et al., 2007
HIF1A	Galbán et al., 2008
VHL	Abdelmohsen et al., 2009
GNL3L	Abdelmohsen et al., 2009
RAB11A	Abdelmohsen et al., 2009
GOLPH4	Abdelmohsen et al., 2009
HDAC4	Abdelmohsen et al., 2009
NCL	Abdelmohsen et al., 2009
ZMAT3	Abdelmohsen et al., 2009
LMNB1	Abdelmohsen et al., 2009
PKN2	Abdelmohsen et al., 2009
KRAS	Abdelmohsen et al., 2009
H2AFV	Abdelmohsen et al., 2009
XPO1	Abdelmohsen et al., 2009
RPP14	Abdelmohsen et al., 2009
BCL9	Abdelmohsen et al., 2009
CA5B	Abdelmohsen et al., 2009
MCM4	Abdelmohsen et al., 2009
ACTG1	de Silanes et al., 2004
UBE2N	de Silanes et al., 2004
MTA1	de Silanes et al., 2004
THBS1	Mazan-Mamczarz et al., 2008
EIF4EBP2	Mazan-Mamczarz et al., 2008_2
BAX	Mazan-Mamczarz et al., 2008_2
CASP2	Mazan-Mamczarz et al., 2008_2
CDK1	Mazan-Mamczarz et al., 2008_2
CDK7	Mazan-Mamczarz et al., 2008_2
RAD51AP1	Mazan-Mamczarz et al., 2008_2
TNFSF12	Mazan-Mamczarz et al., 2008_2
RAB2A	Mazan-Mamczarz et al., 2008_2
PAI2	Maurer et al., 1999
GADD45A	Zhang et al., 2006
ESR1	Hostetter et al., 2008
IL3	Ma et al., 1996

TNF	Dean et al., 2001
SLC11A1	Xu et al., 2005
YES1	Xu et al., 2005
JUND	Zou et al., 2010
XIAP	Zhang et al., 2009
SMN2	Farooq et al., 2009
IL8	Suswam et al., 2005
CTNNB1	de Silanes et al., 2003
CD9	Calaluce et al., 2010
CALM2	Calaluce et al., 2010
CCND3	Rodriguez et al., 2010
FASLG	Drury et al., 2010
CD55	Gray et al., 2010
TUBB3	Raspaglio et al., 2010
CDKN2A	Chang et al., 2010
MARCKS	Wein et al., 2003
TIA1	Pullmann et al., 2007